Petrogenesis of Luchuba and Wuchaba granitoids in Western Qinling: geochronological and geochemical evidence

Juanjuan Kong [a, b,c, *], Yaoling Niu [a, b, d, *], Meng Duan [e], Yu Zhang [f], Yan Hu [a], Jiyong Li [a, b, c], Shuo Chen [a, b, c]

[a] Institute of Oceanology, Chinese Academy of Sciences, Qingdao 266071, China

[b] Laboratory for Marine Geology, Qingdao National Laboratory for Marine Science and Technology, Qingdao 266061, China

[c] University of Chinese Academy of Sciences, Beijing 100049, China

[d] Department of Earth Sciences, Durham University, Durham DH1 3LE, UK

[e] School of Earth Science and Resources, China University of Geosciences, Beijing 100083, China

[f] School of Earth Sciences, Lanzhou University, Lanzhou 730000, China

*Corresponding authors:
Miss Juanjuan Kong, juanjuan0317@ foxmail.com
Professor Yaoling Niu, yaoling.niu@foxmail.com

Address: Institute of Oceanology, Chinese Academy of Sciences, No. 7 Nanhai Road, Shinan District, Qingdao 266071, China. Tel.: +86 0532 82898980

Abstract

The West Qinling Orogenic Belt (WQOB) is a major portion of the Qinling-Dabie-Sulu Orogen and holds essential information for understanding the prolonged evolution of the northeastern branch of the Paleo-Tethys in East Asia. This study focuses on the petrogenesis of granitoids from Luchuba and Wuchaba plutons in the WQOB. We obtained zircon U-Pb ages of 211 ± 1.4Ma for the Luchuba pluton and 218.7 ± 1.3Ma for the Wuchaba pluton, which are the same as the proposed timing of continental collision at ~220Ma. We thus interpret the granitoids to represent a magmatic response to the collision between the North China Craton (NCC) and the Yangtze Block (YB). The two plutons are metaluminous to weakly peraluminous I-type granitoids. Samples from the two plutons show strong light rare earth element (REEs) enrichment and weak heavy REE depletion, with varying negative Eu anomalies, which is most consistent with significant plagioclase fractionation although the possible effect of plagioclase as residual phase in the magma source region cannot be ruled out. In primitive mantle normalized multi-element variation diagrams, nearly all the samples show negative Nb, Ta, P and Ti anomalies and relative enrichment in Rb, Pb, U and K. These characteristics resemble those of the average continental crust. The Luchuba pluton has lower $(^{87}Sr/^{86}Sr)_i$ (0.7051 to 0.7104), higher $\varepsilon_{Nd}(t)$ (-8.11 to -5.73) and $\varepsilon_{Hf}(t)$ (-6.70 to -1.65) than mature continental crust ($[^{87}Sr/^{86}Sr]_i > 0.72$, $\varepsilon_{Nd}(t) < -12$). The Wuchaba pluton also has lower $(^{87}Sr/^{86}Sr)_i$ (0.7069 to 0.7080), higher $\varepsilon_{Nd}(t)$ (-9.86 to -3.34) and $\varepsilon_{Hf}(t)$ (-5.69 to 1.58) than mature continental crust. We conclude that the Luchuba and Wuchaba granitoids in the WQOB are best explained as resulting from fractional crystallization with crustal assimilation of parental magmas derived from melting of Mianlue oceanic crust under amphibolite facies conditions during the initial stage of continental collision between the North China Craton and the Yangtze Block. Mafic magmatic enclaves (MMEs) of Wuchaba pluton are earlier cumulates of the same magmatic system. The Mianlue oceanic crust (MORB-like) contributes to the source of the Luchuba and Wuchaba granitoids, pointing to the significance of melting of oceanic crust for continental crust accretion.

Key words: Western Qinling; Luchuba and Wuchaba granitoids; granitoid petrogenesis; crust accretion.

Introduction

The Qinling Orogen is one of the largest orogenic belts in Asia (Mattauer et al. 1985), linking Kunlun and Qilian orogens to the west and Dabie–Sulu orogen to the east (Meng and Zhang 2000; Ratschbacher et al. 2003), across Central China for ~ 2500 km. It developed through a series of complex seafloor subduction and terrane collision events (Zhang et al. 2001; Ratschbacher et al. 2003; Wang et al. 2009; Wu and Zheng 2012), ultimately completed as the result of the continental collision between the Yangtze Block (YB) and the North China Craton (NCC) along the Mianlue suture zone in the early Mesozoic (see Fig. 1; Dong et al. 2011 and references therein). Abundant granitoids throughout much of the West Qinling were produced during this time period and have received much attention in recent years with mounting geochronological and geochemical data with the aim of better understanding magma sources and processes in the context of studying the Qinling orogenesis. However, the petrogenesis of these granitoids remains controversial (Sun et al. 2002a, b; Wang et al. 2007, 2011; Qin et al. 2009, 2010; Liu et al. 2011a, b; Dong et al. 2011, 2012; Yang et al. 2011, 2012; Xiao et al. 2013), and the debate mainly centers on the sources of these granitoids (e.g., upper crust, lower crust or crust-mantle magma mixing) and the geodynamic evolution.

In this paper, we focus on the Luchuba and Wuchaba granitoid plutons in the central West Qinling Orogenic Belt (WQOB) because of the geological information available due to the associated mineralization and its exploration. Existing models on the petrogenesis of these plutons include: (1) upper crust melting (Ou et al. 2010; Peng 2012, 2013); (2) lower crust melting (Xu et al. 2013); (3) partial melting of Mesoproterozoic crustal rocks and melt

79 interaction with sub-continental lithospheric mantle (SCLM) (the interpreted source of MMEs)
80 (Zhu et al. 2013). The crystallization age of the Wuchaba pluton has been hotly debated to vary
81 from 264 to 213 Ma (Gao et al. 2011; Li et al. 2012; Peng 2012, 2013; Xu et al. 2014; Zeng et
82 al. 2014; Wang et al. 2015) for multi-stage magmatic emplacement with views on tectonic
83 settings varying from subduction-related, syn-collisional to post-collisional (Lu 2004; Li et al.
84 2012). Debates on the petrogenesis and tectonic settings of the Luchuba and Wuchaba
85 granitoids continued. It should be noted that previous studies on the Luchuba and Wuchaba
86 plutons are limited with little systemic chronology, geochemistry and isotopic data. Here we
87 present new LA-ICP-MS zircon U-Pb ages, bulk-rock major and trace element data and Sr–
88 Nd–Hf isotopic compositions to discuss the petrogenesis of these two granitoid plutons in the
89 context of geodynamic evolution.

90 **Geological setting and samples**

91 The Qinling orogenic belt is adjacent to the Qilian orogenic belt (Fig. 1a) and is bounded by
92 the Linxia–Wushan–Tianshui fault to the north and the Mianlue suture in the south (Fig. 1b).
93 The Qinling orogen has been divided into East and West Qinling on the basis of their geological
94 differences (Zhang et al. 2001, 2005, 2007; Feng et al. 2002) (Fig. 1b). The granitoids with
95 ages of 245–200 Ma are distributed between the Shangdan and Mianlue sutures along an
96 approximately E-W trending zone (Zhu et al. 2011; Dong et al. 2011). The WQOB is interpreted
97 as having undergone supercontinent breakup, Qinling-Qilian-Kunlun seafloor spreading and
98 subduction, continent-continent collision and intraplate processes since the Neoproterozoic
99 (Xu et al. 2014).

100 In the WQOB, the Phanerozoic strata are mostly Devonian-Cretaceous sedimentary units

101 with minor Cambrian-Silurian sedimentary units. The Precambrian basement is rarely exposed
102 (Feng et al. 2002). Zhang et al. (2007) confirm that the basement of the WQOB has affinities
103 with the Yangtze block. The Luchuba pluton crops out over an area of ~117 km^2, intruding
104 Devonian and Carboniferous limestone, sandstone and shale (Ou et al. 2010). The Wuchaba
105 pluton, also known as Zhongchuan pluton, has a circular shape with an outcrop area of ~210
106 km^2 (Zeng et al. 2012), intruding the Middle Devonian Shujiaba group ($D2sh^1$) and
107 Carboniferous Xiajialing group (C1x) (Fig. 1c). In the field, the Luchuba granitoids are light
108 grey, and structurally massive with medium-grained or porphyritic texture (Fig. 2a). The
109 Wuchaba granitoids (Fig. 2b) are light red and smoky gray in color, with medium-to coarse-
110 grained and porphyritic texture. Mafic magmatic enclaves (MMEs) occur locally in both
111 Luchuba and Wuchaba plutons, exhibit angular to oval shapes and varying size (10 to 20 cm
112 in diameter), and have no chilled margins with the host granitoids (Fig. 2a, b).

113 The Luchuba granitoids are mainly composed of granodiorite (Fig. 3a) and biotite
114 monzogranite (Fig. 3b), and have porphyritic texture with the mineral assemblage of
115 plagioclase (~30 to 40%) + K-feldspar (~10 to 20%) + quartz (~30 to 40%) with total biotite +
116 hornblende (~5 to 10%). The Wuchaba pluton mainly includes biotite monzogranite (Fig. 3c),
117 biotite granite and diorite with the mineral assemblage similar to that of the Luchuba pluton.
118 The mineralogy is dominantly plagioclase (~30%), quartz (~20%), K-feldspar (~30 to 40%)
119 with minor hornblende and biotite (~10% in total) and accessory minerals such as apatite,
120 zircon and Fe-Ti oxides. The MMEs are fine-grained and show equigranular and
121 hypidiomorphic textures. It is important to note that the MMEs share the same mineralogy with
122 the more felsic hosts but have greater modes of mafic minerals (~55% hornblende and biotite)

and lesser plagioclase (~20%), quartz (~10%) and K-feldspar (~10%) (Fig. 3d and Fig. 3e). Acicular apatite is ubiquitous in the MMEs (Fig. 3f). Euhedral to subhedral plagioclase crystals occur either as phenocrysts or as elongate laths. Quartz commonly occurs as anhedral grains. K-feldspar is mainly megacrysts. Apatite and hornblende display euhedral habit.

Analytical methods

In this study, 24 representative samples (including 2 host-MME pairs) from the Luchuba and Wuchaba plutons were analyzed for whole-rock major and trace elements, three of these representative samples were selected for zircon U-Pb dating. Fifteen of these samples were analyzed for whole-rock Sr-Nd-Hf isotope compositions. Weathered surfaces were removed and thoroughly cleaned, then ultrasonically cleaned with Milli-Q water and dried before the material was powdered to less than 200-mesh in a clean environment using an agate mill for analysis.

LA-ICP-MS zircon U–Pb dating

Zircons were extracted using combined techniques of heavy liquid and magnetic separation. The zircon internal structure was examined using cathodoluminescence (CL) imaging on an EMPA-JXA-8100 scanning electron microscope at China University of Geosciences, Wuhan (CUGW) (Fig. 4). Zircon U-Pb dating on samples SEB12-01, YDB12-05 and DPC12-01 was carried out at the Geologic Lab Center, China University of Geosciences, Beijing (CUGB) using an Agilent 7500a inductively coupled plasma mass spectrometer (ICP-MS) with New Wave UPP-193 laser ablation system. During the analysis, laser spot size was set to ~36 μm for most analyses and to 25μm for metamorphic rims with laser energy density set at 8.5 J/cm^2 and repetition rate at 10 Hz. The procedure of laser sampling is 5s pre-ablation, 20s sample-

chamber flushing and 40s sampling ablation. The ablated material is carried into the ICP-MS by the high-purity Helium gas stream with a flux of 0.8 L/min. The whole laser path was fluxed with N_2 (15 L/min) and Ar (1.15 L/min) in order to increase energy stability. The counting time for U, Th, ^{204}Pb, ^{206}Pb, ^{207}Pb and ^{208}Pb is 20 ms, and is 15 ms for other elements. Calibrations for the zircon analyses were carried out using NIST 610 as an external standard and Si as internal standard. U-Pb isotope fractionation effects were corrected for using zircon 91500 (Wiedenbeck et al. 1995) as external standard. The data were processed using the GLITTER4.41 program with common Pb correction done following Andersen (2002) and analytical details described in Song et al. (2010a). The age data are given in Table 2 and the concordia diagrams and weighted mean age calculations were done using ISOPLOT 4.15 (Ludwig 2012; Fig. 5).

Major and trace elements

Whole-rock major and trace elements were analyzed using Prodigy Inductively Coupled Plasma Optical Emission Spectrometer (ICP-OES) and Agilent 7500a ICP-MS, respectively at CUGB. Analyses of United States Geological Survey (USGS) rock standards (AGV-2 and GSR-1) and Chinese national rock standard (GSR-3) give precision and accuracy better than 5% (2σ) for major elements and 10% (2σ) for trace elements. Analytical details are given in Song et al. (2010b).

Sr–Nd–Hf isotopes

For Sr, Nd and Hf isotope analyses, about 100 mg of sample powder was dissolved in a HF + HNO_3 mixture in Teflon beakers. The Sr, Nd and Hf were then separated using cation-exchange techniques. The Sr isotope reatios were measured using a Finnigan Triton Thermal Ionization

Mass Spectrometer (TIMS) and the Hf and Nd isotope ratios were measured using Multi-Collector Inductively Coupled Plasma Mass Spectrometry (MC-ICP-MS) at Guangzhou Institute of Geochemistry. The $^{87}Sr/^{86}Sr$, $^{143}Nd/^{144}Nd$ and $^{176}Hf/^{177}Hf$ ratios are reported as values normalized to $^{86}Sr/^{88}Sr$ of 0.1194, $^{146}Nd/^{144}Nd$ of 0.7219 and $^{179}Hf/^{177}Hf$ of 0.7325, respectively. During our analysis, repeated analyses of the NBS-987 Sr standard yielded $^{87}Sr/^{86}Sr = 0.710287 \pm 20$ (n = 21, 2σ) and JNdi-1 Nd standard gave $^{143}Nd/^{144}Nd$ 0.512086 ± 16 (n = 11, 2σ). Analyses of Hf standard yielded $^{176}Hf/^{177}Hf$ of 0.283099 ± 15 (n = 13, 2σ) for BHVO-2 and 0.283216 ± 15 (n = 6, 2σ) for JB-3, which are consistent with the reference values (Raczek et al. 2003, Li et al. 2010). Sample preparation procedures and analytical details are described in Wei et al. (2002) and Li et al. (2004, 2005).

Results

Zircon U–Pb data

Zircon cathodoluminescence (CL) images are shown in Fig. 4. Most zircons are euhedral with oscillatory or linear zoning, ranging from 100 to 300μm in length with variable Th (65 to 805 ppm), U (175 to 3300 ppm) and Th/U ratio (0.058 to 1.04), which is consistent with a magmatic origin (Rubatto and Gebauer 2000; Corfu et al. 2003; Hanchar and Hoskin 2003; Cao et al. 2011).

Thirty grains of zircon from sample SEB12-01 of the Luchuba pluton were analyzed (Table 1). Three spots were excluded in the age calculation because of their high ^{204}Pb and significant deviation from the concordia. Twenty-seven spots form a cluster giving a weighted mean $^{206}Pb/^{238}U$ age of 211 ± 1.4 Ma (MSWD = 1.4, n = 27) (Fig. 5a). All the 24 zircon grains from sample YDB12-05 of the Luchuba pluton plot close to the concordia curve (Fig. 5b). Two

189 grains give younger ages of 195 Ma and 196 Ma probably due to Pb loss. Other grains give a
190 weighted mean $^{206}Pb/^{238}U$ age of 218.5 ± 2.3Ma (MSWD = 2.9, n = 22). Twenty zircons from
191 sample DPC12-01 of the Wuchaba pluton give a weighted mean $^{206}Pb/^{238}U$ age of 218.3 ±
192 1.7Ma (MSWD = 0.56, n = 20) (Fig. 5c). All these are interpreted as crystallization ages of the
193 two plutons. The two distinct ages of 211 ± 1.4 Ma and 218.5 ± 2.3 Ma of the Luchuba pluton
194 suggests prolonged magmatism during the same event.

195 *Major and trace elements*

196 Whole-rock major and trace element compositions of the granitoids and MMEs from the
197 Luchuba and Wuchaba plutons are given in Table 2. The Luchuba granitoids show varying SiO_2
198 (64.15 to 75.82wt.%) as do the Wuchaba granitoids (64.61 to 73.91wt.% SiO_2). In the K_2O +
199 Na_2O vs. SiO_2 diagram (Fig. 6), most of the samples from the Luchuba and Wuchaba granitoids
200 display a roughly continuous compositional spectrum from granodiorite to granite in
201 subalkaline field with aluminum saturation index ([ASI = molar Al_2O_3/ ($CaO + K_2O + Na_2O$)])
202 ≤ 1.10 (Fig. 7). They exhibit a high K character with high K_2O/Na_2O (1.02 to 1.32 for Luchuba
203 and 1.11 to 2.28 for Wuchaba plutons, Table 3). The high K_2O sample (MZG12-02) has high
204 modal biotite and K-feldspar (~30%), while the low K_2O sample (CJM12-01(host)) has few
205 modal biotite and K-feldspar (< 5%). In SiO_2 variation diagrams (Fig. 8), most samples from
206 the two plutons define a roughly correlated evolution trend: Al_2O_3, CaO, Fe_2O_3, MgO, TiO_2,
207 P_2O_5, Sr, Eu and Yb decrease with increasing SiO_2 whereas Na_2O and K_2O increase with
208 increasing SiO_2. The Luchuba granitoids display strongly fractionated REE patterns ($(La/Yb)_N$
209 = 5.28 to 18.84) with moderately negative Eu anomalies (Eu/Eu* = 0.41 to 0.83) (Fig. 9a). The
210 Wuchaba granitoids show moderate to strong LREE enrichment ($(La/Yb)_N$ = 4.13 to 34.61) and

211 variable negative Eu anomalies (Eu/Eu* = 0.16 to 0.86; Fig. 9c). Samples from the Luchuba
212 and Wuchaba plutons have low Sr content and significant negative Sr anomalies (Sr/Sr* =
213 $2Sr_N/[Pr_N + Nd_N]$), corresponding to its significant negative Eu anomalies (Fig. 10), which is
214 most consistent with significant plagioclase fractionation although the possible effect of
215 plagioclase as residual phase in the magma source region cannot be ruled out. In the trace
216 element spider diagrams, all the samples show negative Nb, Ta, P and Ti anomalies and Rb, Th,
217 U and K enrichment (Fig. 9b, d). These characteristics resemble those of bulk continental crust
218 (BCC; Rudnick and Gao 2003).

219 The MMEs from the Wuchaba pluton have relatively lower SiO_2 contents (53.31 and
220 53.92 wt.%; Figs. 6, 8) and show the same composition in the TAS diagram (Fig. 6). The MMEs
221 have negative Eu anomalies with Eu/Eu* of 0.26 and 0.65, displaying higher abundances of
222 HREEs (Fig. 9c) and higher Nb/Ta (17.52 and 17.38) than the host, which is consistent with
223 higher modal contents of hornblende (Foley et al. 2000; Niu and O'Hara 2009; Chen et al. 2015,
224 2016).

225 *Sr-Nd-Hf isotopes*

226 Whole rock Sr-Nd-Hf isotope data for 15 samples (including two MMEs) of the two plutons
227 are given in Table 3 and plotted in Figs. 11-13. The $I_{Sr}(t)$, $\varepsilon_{Nd}(t)$ and $\varepsilon_{Hf}(t)$ refer to the age (t =
228 220 Ma) corrected values. All the analyzed Luchuba samples have variable values of $I_{Sr}(t)$
229 (0.7052 to 0.7104), $\varepsilon_{Nd}(t)$ of -8.11 to -5.73 and $\varepsilon_{Hf}(t)$ of -6.70 to -1.65. The Wuchaba pluton has
230 the isotopic characteristics of $I_{Sr}(t)$ = 0.7069 to 0.7080, $\varepsilon_{Nd}(t)$ = -9.86 to -3.34 and $\varepsilon_{Hf}(t)$ = -5.69
231 to 1.58. The two MMEs of Wuchaba granitoids also show Sr-Nd-Hf isotopic compositions ($I_{Sr}(t)$
232 is 0.7069 and 0.7073, $\varepsilon_{Nd}(t)$ = -4.74 and -3.34, $\varepsilon_{Hf}(t)$ = -0.78 and 1.58) comparable to those of

233 Wuchaba host. Sample ZKL12-01 of the Luchuba pluton gives very high $^{87}Sr/^{86}Sr$ of 0.737981.
234 This high ratio is consistent with the high Rb/Sr ratio resulting from significant extent of
235 plagioclase-dominated fractional crystallization (also low in Ba, P, and Ti; see Fig. 9). The high
236 $^{87}Rb/^{86}Sr$ ratio (10.50) makes the calculated $I_{Sr}(t)$ unreliable (Jahn et al. 2000).

237 **Discussion**

238 *Assimilation and Fractional crystallization (AFC)*

239 The data shown in SiO_2-variation diagrams (Fig. 8) are to a first-order consistent with varying
240 extent of fractional crystallization of hornblende, plagioclase, Fe–Ti oxides and apatite.
241 However, these trends are also consistent with modal variations of these phases in the samples
242 although the depletion in P, Nb, Ta and Ti emphasizes the significance of fractional
243 crystallization. These granitoids display sub-chondritic Nb/Ta ratio, which is also consistent
244 with hornblende controlled fractionation ($Kd_{\text{hornblende}}$ Nb/Ta = 1.40) (Foley et al. 2002). The
245 moderately to strongly negative anomalies of Ba, Sr and Eu (Fig. 9 and Fig. 10) indicate
246 extensive fractionation of plagioclase and/or K-feldspar (Wu et al. 2003). The scattered data in
247 the I_{Sr} vs. 1/Sr and $\varepsilon_{Nd}(t)$ vs. 1/Nd plots (Fig. 11) suggest that the petrogenesis of samples from
248 the two plutons was controlled by fractional crystallization and contamination (Xing et al.
249 1996). While scattered, it is apparent in Fig. 12 that the two plutons show quite similar range
250 of initial $^{87}Sr/^{86}Sr$ values (except for sample ZKL12-01 with high Rb/Sr) while the $\varepsilon_{Nd}(t)$ and
251 $\varepsilon_{Hf}(t)$ values decrease with increasing SiO_2, which is consistent with fractional crystallization,
252 accompanied by increased crustal contamination/assimilation. It is should be noted that the
253 small variation of Sr isotopes reflects similar Sr isotope composition of the actually
254 contaminated crust. All these data signify that assimilation–fractional crystallization (AFC)

processes (DePaolo 1981) played a role in the petrogenesis of the two plutons.

Petrogenesis of granitoids

Generally, granitoids are typically divided into I-, S-, A- and M-type in terms of source rock types and petrogenesis (e.g., Chappell et al. 1974; Collins et al. 1982; Whalen 1985). Amphibole, cordierite, and alkaline minerals are important diagnostic minerals for discriminating I-, S- and A-type granites respectively. The absence of aluminous minerals such as muscovite, tourmaline and garnet, combined with the magmatic assemblage of hornblende and biotite (Fig. 3), and the relatively low A/CNK values (<= 1.1, Fig. 7) is consistent with these granitoids being of I-type.

The Luchuba and Wuchaba plutons have low $(La/Yb)_N$ and Sr/Y, suggesting that their parental magmas were generated under relatively low pressures (~ 40 km) without garnet being present as the residual phase in the magma source region or as liquidus phase during magma evolution (e.g., Martin et al. 2005; Klein et al. 2000; Pertermann et al. 2004). Here we emphasize a maximum depth of ~40 km for melt formation because of the lack of garnet signature in the two granitoid plutons (Mo et al. 2008).

Partial melting of the lower continental crust may account for the origin of granitic rocks, and some authors argued that the magma sources for the WQOB granitoids could be basic rocks (amphibolite) (Zhang et al. 2007). However, the dehydration melting of amphibolite in the lower crust should result in melts high in Na_2O and low in K_2O (Beard and Lofgren 1991), which is inconsistent with the high-K characteristics of the Luchuba and Wuchaba plutons. Besides, partial melting of the basaltic source usually needs higher melting temperature and amphibole dehydration melting cannot produce such volumetrically significant granitoids.

277 Thus, the origin by partial melting of pre-existing mafic lower crust is less likely. The Luchuba
278 and Wuchaba plutons, as other coeval granites elsewhere in the WQOB, have lower $(^{87}Sr/^{86}Sr)_i$,
279 higher $\varepsilon_{Nd}(t)$ and $\varepsilon_{Hf}(t)$ than the mature continental crust ($[^{87}Sr/^{86}Sr]_i > 0.72$, $\varepsilon_{Nd}(t) < -12$) (Fig.
280 13a) (Zhang et al. 2007). Hence, it is unlikely that these granitoids were produced by melting
281 of mature continental crust (upper crust) ($[^{87}Sr/^{86}Sr]_i > 0.72$, $\varepsilon_{Nd}(t) < -12$) (Niu et al. 2009), but
282 has significant mantle contribution (or juvenile crustal material) in terms of isotopes. In
283 addition, Hf-Nd isotopes are coupled and lie in the global mantle and crustal array (Fig. 13b)
284 indicating mantle (or juvenile continental crust) contribution. In the age-$\varepsilon_{Hf}(t)$ diagram (Fig.
285 13c), the majority of samples fall between the mantle and crustal evolution line, also indicating
286 significant mantle contribution for these granitoids (Wang et al. 2012). Additionally, pioneering
287 studies (Dong et al. 2011, 2012) suggest that the Paleo-Tethys Mianlue Ocean was already
288 closed at the time of granitoids emplacement (~ 220Ma). Therefore, we suggest that the
289 Luchuba and Wuchaba plutonism was a response to continental collision. In the context of
290 continental collision, reasonable mechanism for granitoid magmatism with significant mantle
291 isotopic signature was discussed by Niu et al. (2013). Partial melting of subducted basaltic
292 ocean crust (Mianlue MORB) under amphibolite facies conditions can produce andesitic melts
293 resembling bulk continental crust (BCC) (Niu et al. 2013; also see below). Note that the lack
294 of adakite signature (i.e., high Sr/Y and La/Yb; Defant and Drummond 1990; Castillo 2006
295 2012) requires melting under amphibolite facies conditions (see Niu et al. 2013). In this study,
296 the Luchuba and Wuchaba plutons have REE and trace element patterns resembling those of
297 the BCC (Fig. 9). Despite the felsic compositions with radiogenic Sr and unradiogenic Nd of
298 the Luchuba and Wucbaba plutons, they have higher $\varepsilon_{Nd}(t)$ value than typical continental crust,

299 especially their high $\varepsilon_{Hf}(t)$ values are close to zero (see above). Simple isotopic mixing
300 calculations suggest that ~ 50% ocean crust (MORB) contributes to the source of the Luchuba
301 and Wuchaba plutons (Fig. 14). Hence, the syncollisional plutons represent juvenile crust with
302 primary materials isotopically coming from the mantle. In this case, the remaining part of the
303 Mianlue oceanic crust is most likely the best source for generating andesitic magmas parental
304 to the Luchuba and Wuchaba plutons; partial melting of the basaltic oceanic crust produces
305 felsic melts and the ocean crust derived from the mantle not long ago imparts the mantle
306 isotopic signature (Niu et al. 2013). Meanwhile, AFC during magma ascent can explain the
307 crustal signatures of the Luchuba and Wuchaba granitoids.

308 *Origin of MMEs*

309 Both Luchuba and Wuchaba plutons contain mafic magmatic enclaves (MMEs). The origin of
310 the MMEs is key to the petrogenesis of the granitoids. Three models have been proposed to
311 explain the origin of MMEs: (1) restites (Chen et al. 1989; Chappell et al. 2000); (2)
312 representing mantle derived melts (Barbarin 2005; Mo et al. 2007; Yang et al. 2007; Clemens
313 and Stevens 2011); (3) mafic cumulate of the same magmatic system with the host (Wall et al.
314 1987; Dahlquist 2002; Niu et al. 2013; Huang et al. 2014; Chen et al. 2015, 2016). The MMEs
315 in the Wuchaba pluton (1) have the same magmatic mineralogy as the host and a fine-grained
316 texture without any disequilibrium features such as crystal resorption or reactive overgrowth
317 (Fig. 3d), which, together with lacking metamorphic or residual sedimentary fabrics, rules out
318 the restite origin; (2) the similar U-Pb ages of both MMEs and the host (e.g., Zhu et al. 2013)
319 also argue against the restite model; (3) the MMEs have greater amphibole modes with
320 cumulate texture formed by hornblende-plagioclase; (4) MMEs have slightly higher $\varepsilon_{Nd}(t)$ or

321 $\varepsilon_{Hf}(t)$ than their host granitoids and have similar Sr isotopes (Fig. 12). The similar isotope
322 variation ranges for both granitoid hosts and the MMEs are inconsistent with mafic-felsic
323 magma mixing, but are consistent with the same mantle source with varying extents of crustal
324 contamination as discussed above (Figs. 11-12).

325 Many authors still follow the popular view that the similar Sr-Nd-Hf isotope between the
326 host and MMEs have resulted from magma mixing. We emphasize that it is physically unlikely
327 that isotopes become homogenized whereas major and trace elements are not (Niu et al. 2013;
328 Chen et al. 2015). It also should be noted that the MMEs and host rocks have significant linear
329 trends in SiO_2 variation diagrams (Fig. 8), which could be interpreted as magma mixing, but
330 they are more consistent with fractional crystallization with superimposed/enhanced effects of
331 modal mineralogy. It is important to note that the fine grain size of MMEs is no evidence
332 against their cumulate origin, but evidences a cumulate origin at an early stage of magma
333 cooling when magma was emplaced in a new and relatively cold ambient crust; the first major
334 liquidus phases are amphibole (± biotite ± plagioclase) and rapid quenching will facilitate
335 abundant nucleation without between-nuclei space for growth, thus forming fine-grained MME
336 cumulates (Chen et al. 2015). Therefore, we maintain that the MMEs represent disturbed earlier
337 cumulate of the same magmatic system.

338 *Geodynamic Implications*

339 The Qinling orogenic belt culminated with the collision of the Yangtze Block (YB) with the
340 North China Craton (NCC) in the Mid-Late Triassic along the Mianlue suture zone (Chen et al.
341 2000, 2010; Liu et al. 2005; Jiang et al. 2010; Li et al. 2011; Dong et al. 2011, 2012, 2013,
342 2016; Ni et al. 2012). The age data show that the NCC-YB collision occurred between 234 and

220 Ma (Sun et al. 2002a; Zhu et al. 2009; Qin et al. 2010; Liu et al. 2011; Dong et al. 2012; Li et al. 2013, 2015). The Luchuba and Wuchaba granitoids have identical crystallization ages to other late Triassic granitoids in the WQOB (Zhang et al. 2007). The popular explanation is that slab break off along the Qinling-Dabie orogen occurred at shallow depth causing asthenosphere upwelling and lower crust melting causing widespread Triassic granitoid magmatism (Sun et al. 2002a). However, it is physically difficult to have asthenosphere upwelling without significant mantle lithosphere delamination (removal) and lower crust melting. In fact, continuous lithosphere extension and delamination in the WQOB occurred at < 210 Ma (Yang et al. 2012). Other authors postulated a thermal pulse associated with the slab break off resulting from the asthenosphere upwelling along the Mianlue suture during the Late Triassic; the upwelling triggered partial melting of the Neoproterozoic SCLM that generated the MME and the partial melting of the Neo-Mesoproterozoic lower crust for the granitic magmatism (Qin et al. 2009; Zhu et al. 2013). The MMEs are of cumulate origin with the hornblende-plagioclase assemblage of the same magmatic system as the host granitoid rather than representing mafic magmas of SCLM origin (see Huang et al. 2014; Chen et al. 2015, 2016). Hence, partial melting of Mesoproterozoic crustal rocks and melt interaction with sub-continental lithospheric mantle (SCLM) is also implausible.

The magma emplacement ages for the Luchuba and Wuchaba granitoids broadly coincide with the timing of the NCC-YB collision. It is remarkable that the Nb-Ta-Ti depletion and the subchondritic Nb/Ta ratio are characteristic of these granitoids without invoking active subduction-zone magmatism; subduction-related magmatism would produce variably high excess Sr that is inconsistent with the Sr deficiency of the granitoids (Fig. 9). Therefore, we

365 suggest that in the late Triassic the WQOB witnessed a period of syn-collisional granitoid
366 magmatism not subduction-related magmatism. The following scenario is proposed to explain
367 the petrogenesis of the Luchuba and Wuchaba granitoids.

368 We argue that the YB-NCC collision began at ~220 Ma (Fig. 15) and finished ~210 Ma
369 (see discussion above). Upon collision, the Mianlue oceanic crust (as old as ~350 Ma; Xu et al.
370 2002) that had been subducted beneath the Qinling active (Andean-type) continental margin
371 (Dong et al. 2012) may have undergone melting producing the melts parental to the Luchuba
372 and Wuchaba granitoids. It is possible and likely that the Mianlue oceanic crust reached
373 temperatures in excess of 800 °C with continued underthrusting to produce significant amounts
374 of melt. Because during Triassic subduction to collision hot thermal conditions prevailed at an
375 active continental margin with a geotherm >20 °C/km well within the melting conditions
376 (Kelemen et al. 2003). Therefore, the remaining Mianlue oceanic crust was continuously and
377 slowly subducted along high T/P paths (as attaining thermal equilibrium with the superjacent
378 hot active continental margin) resulting in enhanced heating at the early stage of YB-NCC
379 collision.The underthrusting Mianlue ocean crust began to melt when passing through the
380 hydrous basaltic/granitic solidus (<650 °C) under amphibolite facies conditions (Mo et al. 2008,
381 Niu et al. 2013). Such conditions and processes can produce andesitic melts parental to the
382 Luchuba and Wuchaba granitoids. It is noteworthy that we emphasized melting of MORB under
383 amphibolite facies conditions not amphibole dehydration melting which requires much higher
384 temperature (>850°C, Rushmer 1991). The latter can hardly produce volumetrically significant
385 granitoids (see above). These granitoids resemble the composition of the BCC without the Y
386 or HREE depleted “garnet signature”, in support of melting under amphibolite facies conditions

387 without garnet present as a residual phase (details see Section 3.2.3 in Niu et al. 2013). The
388 andesitic parental magma when emplaced in a magma chamber would rapidly cool and
389 crystallize mafic minerals (e.g., hornblende, biotite) and plagioclase to form fine-grained
390 cumulates (MMEs), which can be readily disturbed by replenishing magmas, leading to the
391 more mafic cumulate to becoming dispersed as MMEs in the granitoid host. Our model is
392 consistent with open-system magma chamber processes with continued evolution (fractional
393 crystallization)/replenishment accompanied by crustal contamination and assimilation.

394 **Conclusions**

395 (1) Zircon U-Pb dating yields ages of 211 ± 1.4 Ma and 218.5 ± 2.3 Ma for the Luchuba pluton
396 and of 218.7 ± 1.3Ma for the Wuchaba pluton, respectively. This is within the age range of the
397 collision of the Yangtze Block with the North China Craton.

398 (2) The granitoids of the Luchuba and Wuchaba plutons display an enriched LILE and LREE
399 patterns and have variable negative Eu anomalies, which is similar to, but more evolved than,
400 those of bulk continental crust. Our results suggest that the Luchuba and Wuchaba plutons are
401 best explained by melting of amphibolite of MORB protolith (the Paleo-Tethys Mianlue ocean
402 crust) during continental collision, which produced granitic melts with a remarkable
403 compositional similarity to the BCC with inherited mantle-like isotopic compositions modified
404 by AFC process-like assimilation.

405 (3) MMEs of Wuchaba pluton are earlier cumulates of the same magmatic system.

406 (4) Ocean crust (MORB-like) contributes to the source of the Luchuba and Wuchaba granitoids,
407 pointing to the significance of ocean crust melting in contributing to the continental crust
408 accretion.

Acknowledgements

We thank Cui Huixia, Gong Hongmei, Guo Pengyuan, Hu Zhenxing, Liu Jinju, Ma Yuxin, Sun Pu, Sun Wenli, Wang Xiaohong, Ye Lei, Ye Xiaolu and Zhang Guorui for assistance with sample preparation. We particularly thank Su Li for major and trace element analysis and zircon analysis and Ma Jinlong for Sr-Nd-Hf isotope analysis. This work was supported by grants from National Natural Science Foundation of China (41130314, 91014003), Chinese Academy of Sciences, regional and local authorities (Shandong Province and City of Qingdao) and Qingdao National laboratory of ocean sciences and Technology.

References

Andersen T (2002) Correction of common lead in U–Pb analyses that do not report ^{204}Pb. Chem Geol 192:59–79

Bacon CR, Druitt TH (1988) Compositional evolution of the zoned calcalkaline magma chamber of Mount Mazama, Crater Lake, Oregon. Contrib Mineral Petrol 98:224-256

Barbarin B (2005) Mafic magmatic enclaves and mafic rocks associated with some granitoids of the central Sierra Nevada batholith, California: nature, origin, and relations with the hosts. Lithos 80:155-177

Beard J, Lofgren G (1991) Partial melting of basaltic and andesitic greenstones and amphibolites under dehydration melting and water-saturated conditions at 1, 3, and 6.9 kilobars. J Petrol 32:365-401

Blichert-Toft J, Albarède F (1997) The Lu-Hf isotope geochemistry of chondrites and the evolution of the mantle-crust system. Earth and Planetary Science Letters 148:243-258

Cao XF, Lü XB, Yao SZ, Mei W, Zou XY, Chen C, Liu ST, Zhang P, Su YY, Zhang B (2011) LA–ICP–MS U–Pb zircon geochronology, geochemistry and kinetics of the Wenquan ore-bearing granites from West Qinling, China. Ore Geol Rev 3:120-131

437 Castillo P R (2006) An overview of adakite petrogenesis. Chin Sci Bull 51:257-268
438 Castillo P R (2012) Adakite petrogenesis. Lithos 134:304-316
439 Chappell BW, White AJR (1974) Two contrasting granite types. Pacific Geol 8:173-174
440 Chappell BW, White AJR, Williams IS, Wyborn D, Wyborn LAI (2000) Lachlan Fold Belt
441 granites revisited: high- and low-temperature granites and their implications. Aust J Earth
442 Sci 47:123–138
443 Chauvel C, Lewin E, Carpentier M, Arndt NT, Marini JC (2008) Role of recycled oceanic basalt
444 and sediment in generating the Hf–Nd mantle array. Nature Geoscience 1: 64-67
445 Chen YD, Price RC, White AJR (1989) Inclusions in Three S-Type Granites from Southeastern
446 Australia. Journal of Petrology 30:1181-1218
447 Chen YJ, Li C, Zhang J, Li Z, Wang HH (2000) Sr and O isotopic characteristics of porphyries
448 in the Qinling molybdenum deposit belt and their implication to genetic mechanism and
449 type. Sci China Ser D 43:82–94 (Suppl.)
450 Chen YJ (2010) Indosinian tectonic setting, magmatism and metallogenesis in Qinling Orogen,
451 central China. Geology in China 37:854–865 (in Chinese with English abstract)
452 Chen S, Niu YL, Sun WL, Zhang Y, Li JY, Guo PY, Sun P (2015) On the origin of mafic
453 magmatic enclaves (MMEs) in syn-collisional granitoids: evidence from the Baojishan
454 pluton in the North Qilian Orogen, China, Miner Petrol:1-20
455 Chen S, Niu YL, Li JY, Sun WL, Zhang Y, Hu Y, Shao FL (2016) Syn-collisional adakitic
456 granodiorites formed by fractional crystallization: Insights from their enclosed mafic
457 magmatic enclaves (MMEs) in the Qumushan pluton, North Qilian Orogen at the northern
458 margin of the Tibetan Plateau. Lithos 248: 455-468
459 Clemens JD, Stevens G (2011) What controls chemical variation in granitic magmas. Lithos
460 134-135:317-329
461 Collins WJ, Beams SD, White AJR, Chappell BW (1982) Nature and origin of A-type granites
462 with particular reference to southeastern Australia. Contrib Mineral Petrol 80:189-200
463 Corfu F, Hanchar JM, Hoskin PWO, Kinny P (2003) Altas of zircon textures. Rev Mineral
464 Geochem 53:469–500
465 Dahlquist J (2002) Mafic microgranular enclaves: Early segregation from metaluminous

magma (sierra de Chepes), Pampean Ranges, NW Argentina. J South Am Earth Sci 15:643-655

Defant M J, Drummond M S (1990) Derivation of some modern arc magmas by melting of young subducted lithosphere. Nature 347:662-665

Depaolo D J (1981) Trace element and isotopic effects of combined wallrock assimilation and fractional crystallization. Earth Planet Sci Lett 53:189-202

Dong YP, Zhang GW, Neubauer F, Liu XM, Genser J, Hauzenberger C (2011) Tectonic evolution of the Qinling orogen, China: review and synthesis. J Asian Earth Sci 41:213-237

Dong YP, Liu XM, Zhang GW, Chen Q, Zhang XN, Li W, Yang C (2012) Triassic diorites and granitoids in the Foping area: Constraints on the conversion from subduction to collision in the Qinling orogen, China. J Asian Earth Sci 47:123-142

Dong YP, Liu XM, Neubauer F, Zhang GW, Tao N, Zhang YG, Zhang, XN, Li W (2013) Timing of Paleozoic amalgamation between the North China and South China Blocks: evidence from detrital zircon U-Pb ages. Tectonophysics 586:173-191

Dong YP, Santosh M (2016) Tectonic architecture and multiple orogeny of the Qinling Orogenic Belt, Central China. Gondwana Res 29:1-40

Feng YM, Cao XZ, Zhang EP, Hu YX, Pan XP, Yang JL, Jia QZ, Li WM (2002) Structure, orogenic processes and geodynamic of the western Qinling orogen (in Chinese). Xi'an map press, Xi'an, pp 1–263

Foley SF, Barth MG, Jenner GA (2000) Rutile/melt partition coefficients for trace elements and an assessment of the influence of rutile on the trace element characteristics of subduction zone magmas. Geochim Cosmochim Acta 64:933-938

Foley S, Tiepolo M, Vannucci R (2002) Growth of early continental crust controlled by melting of amphibolite in subduction zones. Nature 417:837–840

Gao T (2011) The LA-ICP-MS zircon U-Pb dating, geology and geochemistry, tectonic setting of several important intrusions from the north part of the western stage of west Qinling and their relationship with mineralization. PhD thesis, Chang'an University, Xi'an, China

Hanchar JM, Hoskin PWO (2003) Zircon. Rev Mineral Geochem 53:1-500

Higuchi H, Nagasawa H (1969) Partition of trace elements between rock-forming minerals and the host volcanic rocks. Earth Planet Sci Lett 7:281-287

Huang H, Niu YL, Nowell G, Zhao ZD, Yu XH, Zhu DC, Mo XX, D S (2014) Geochemical constraints on the petrogenesis of granitoids in the East Kunlun Orogenic belt, northern Tibetan Plateau: Implications for continental crust growth through syn-collisional felsic magmatism. Chem Geol 370:1-18

Jahn BM, Wu FY, Chen B, (2000) Massive granitoid generation in central Asia: Nd isotopic evidence and implication for continental growth in the Phanerozoic. Episodes 23:82-92

Jiang YH, Jin GD, Liao SY, Zhou Q, Zhao P (2010) Geochemical and Sr-Nd-Hf isotopic constraints on the origin of Late Triassic granitoids from the Qinling orogen, central China: Implications for a continental arc to continent-continent collision. Lithos 117:183–197

Kelemen PB, Rilling JL, Parmentier E, Mehl L, Hacker BR (2003) Thermal structure due to solid-state flow in the mantle wedge beneath arcs. Geophys Monogr Am Geophys Union 138:293-311

Klein M, Stosch HG, Seck H, Shimizu N, (2000) Experimental partitioning of high field strength and rare earth elements between clinopyroxene and garnet in andesitic to tonalitic systems. Geochim Cosmochim Acta 64:99-115

Li N, Chen YJ, Fletcher IR, Zeng QT (2011) Triassic mineralization with Cretaceous overprint in the Dahu Au-Mo deposit, Xiaoqinling gold province: Constraints from SHRIMP monazite U-Th–Pb geochronology. Gondwana Res 20:543-552

Li T, Xu XY, Chen JL, Wang HL, Li ZP, Zhang X (2012) LA-ICP-MS zircon U-Pb dating and tectonic setting of Zhongchuan intrusion, Lixian area, West Qinling orogen. Geol Bull 31:875-883

Li XH, Liu DY, Sun M, Li WX, Liang XR, Liu Y (2004) Precise Sm–Nd and U–Pb isotopic dating of the supergiant Shizhuyuan polymetallic deposit and its host granite, SE China. Geol Mag 141:225-231

Li XH, Qi CS, Liu Y, Liang XR, Tu XL, Xie LW, Yang YH (2005) Rapid separation of Hf from rock samples for isotope analysis by MC-ICPMS: a modified single-column extraction chromatography method. Geochimica 34:109-114

Li XH, Long WG, Li QL, Liu Y, Zheng YF, Yang YH, Chamberlain KR, Wan DF, Guo CH,

525 Wang XC, Tao H (2010) Penglai zircon megacrysts: a potential new working reference
526 material for microbeam determination of Hf–O isotopes and U–Pb age. Geostand Geoanal
527 Res 34:117-134
528 Li XW, Mo XX, Yu XH, Ding Y, Huang XF, Wei P, He WY (2013) Petrology and
529 geochemistry of the early Mesozoic pyroxene andesites in the Maixiu Area, West Qinling,
530 China: products of subduction or syn-collision? Lithos 172/173:158–174
531 Li XW, Mo XX, Huang XF, Dong GC, Yu XH, Luo MF, Liu YB (2015) U–Pb zircon
532 geochronology, geochemical and Sr–Nd–Hf isotopic compositions of the early indosinian
533 Tongren pluton in West Qinling: petrogenesis and geodynamic implications. J Asian Earth
534 Sci 97:38-50
535 Liu SF, Steel R, Zhang GW (2005) Mesozoic sedimentary basin development and tectonic
536 implication, northern Yangtze Block, eastern China: record of continent–continent
537 collision. J Asian Earth Sci 25:9-27
538 Liu SW, Li QG, Tian W, Wang ZQ, Yang PT, Wang W, Bai X, Guo RR (2011a) Petrogenesis
539 of Indosinian granitoids in Middle-Segment of South Qinling Tectonic Belt: constraints
540 from Sr–Nd isotopic systematics. Acta Geol Sin Engl 85:610–628
541 Liu SW, Yang PT, Li QG, Wang ZQ, Zhang WY, Wang W (2011b) Indosinian granitoids and
542 orogenic processes in the middle segment of the Qinling orogen, China. Journal of Jilin
543 University (Earth science edition), 41(6):1928-1943
544 Lu Z, Quan JJ, Chen X, Yan DF (2004) Characteristics and geological effects of magmatic
545 activity of the Zhongchuan granite of western Qinling area. Acta Geologica Gan Su 12:25-
546 30
547 Ludwig K (2012) User's manual for Isoplot version 3.75-4.15: a geochronological toolkit for
548 Microsoft. Excel Berkley Geochronological Center Special Publication No. 5
549 Mattauer M, Matte P, Malavieille J, Tapponnier P, Maluski H, Qin XZ, Qin TY (1985) Tectonics
550 of the Qinling belt: Build-up and evolution of eastern Asia. Nature 317(6037): 496-500
551 Martin H, Smithies RH, Rapp R, Moyen JF, Champion D (2005) An overview of adakite,
552 tonalite–trondhjemite–granodiorite (TTG), and sanukitoid: relationships and some
553 implications for crustal evolution. Lithos 79:1-24
554 Meng QR, Zhang GW (2000) Geologic framework and tectonic evolution of the Qinling-Dabie

555 orogen, central China. Tectonophysics 323:183-196
556 Mo XX, Luo ZH, Deng JF, Yu XH (2007) Granitoids and crustal growth in the east-Kunlun
557 orogenic belt. Geological Journal of China Universities 3:403-414 (in Chinese with
558 English abstract)
559 Mo XX, Niu YL, Dong GC, Zhao ZD, Hou ZQ, Zhou S, Ke S (2008) Contribution of
560 syncollisional felsic magmatism to continental crust growth: A case study of the Paleogene
561 Linzizong volcanic succession in southern Tibet. Chem Geol 250:49-67
562 Ni ZY, Chen YJ, Li N, Zhang H (2012) Pb-Sr-Nd isotope constraints on the fluid source of the
563 Dahu Au-Mo deposit in Qinling Orogen, central China, and implication for Triassic
564 tectonic setting. Ore Geol Rev 46:60-67
565 Niu YL, O'Hara MJ (2009) MORB mantle hosts the missing Eu (Sr, Nb, Ta and Ti) in the
566 continental crust: new perspectives on crustal growth, crust–mantle differentiation and
567 chemical structure of oceanic upper mantle. Lithos 112:1-17
568 Niu YL, Zhao ZD, Zhu DC, Mo XX (2013) Continental collision zones are primary sites for
569 net continental crust growth–A testable hypothesis. Earth Sci Rev 127:96-110
570 Ou CS, Yang YC, Wang H, Yang WG (2010) Characteristics and mineralization of Luchuba
571 granite pluton in Lixian. Gansu Science and Technology 017:37-41
572 Peng X (2012) Magmatic consanguinity and tectonic significance of Zhongchuan rock group
573 in western Qinling. MSc thesis, Chang'an University
574 Peng Xuan (2013) Research on homology for the rock group of monzonite granite in the
575 Western Qinling. Northwestern Geology 1:63-80
576 Pertermann M, Hirschmann MM, Hametner K, Günther D, Schmidt MW (2004) Experimental
577 determination of trace element partitioning between garnet and silica-rich liquid during
578 anhydrous partial melting of MORB-like eclogite. Geochem Geophy Geosy 5: 297-391
579 Qin JF, Lai SC, Grapes R, Diwu CR, Ju YJ, Li YF (2009) Geochemical evidence for origin of
580 magma mixing for the Triassic monzonitic granite and its enclaves at Mishuling in the
581 Qinling orogen (central China). Lithos 112:259–276
582 Qin JF, Lai SC, Grapes R, Diwu CR, Ju YJ, Li YF (2010) Origin of Late Triassic high Mg
583 adakitic granitoid rocks from the Dongjiangkou area, Qinling orogen, central China

584 implications for subduction of continental crust. Lithos 120:347-367
585 Raczek I, Jochum KP, Hofmann AW (2003) Neodymium and strontium isotope data for USGS
586 reference materials BCR-1, BCR-2, BHVO-1, BHVO-2, AGV-1, AGV-2, GSP-1, GSP-2
587 and eight MPI-DING reference glasses. Geostand Newslett 27:173-179
588 Ratschbacher L, Hacker BR, Calvert A, Webb LE, Crimmer JC, McWilliams MO, Ireland T,
589 Dong S, Hu J (2003) Tectonics of the Qinling (Central China): tectonostratigraphy,
590 geochronology, and deformation history. Tectonophysics 366:1-53
591 Rubatto D, Gebauer D (2000) Use of cathodoluminescence for U–Pb zircon dating by ion
592 microprobe: some examples from the Western Alps. In: Pagel M, Barbin V, Blanc P,
593 Ohnenstetter D (eds), Cathodoluminescence in Geosciences. Springer, Berlin, pp 373-400
594 Rushmer T (1991) Partial melting of two amphibolites: contrasting experimental results under
595 fluid absent conditions. Contrib Mineral Petrol 107:41-59
596 Rudnick RL, Gao S (2003) Composition of the continental crust. Treatise Geochem 3:1-64
597 Schnetzler CC, Philpotts JA (1970) Partition coefficients of rare-earth elements between
598 igneous matrix material and rock-forming mineral phenocrysts; II. Geochim Cosmochim
599 Acta 34:331-340
600 Shen J, Zhang ZQ, Liu DY (1997) Sm–Nd, Rb–Sr, $^{40}Ar/^{39}Ar$, $^{207}Pb/^{206}Pb$ age of the Douling
601 metamorphic complex from eastern Qinling orogenic belt. Acta Geol Sin 18:248-254
602 Song SG, Niu YL, Wei CJ, Ji JQ, Su L (2010a) Metamorphism, anatexis, zircon ages and
603 tectonic evolution of the Gongshan block in the northern Indochina continent—an eastern
604 extension of the Lhasa Block. Lithos 120:327-346
605 Song SG, Su L, Li XH, Zhang GB, Niu YL, Zhang LF (2010b) Tracing the 850-Ma continental
606 flood basalts from a piece of subducted continental crust in the North Qaidam UHPM belt,
607 NW China. Precambrian Res 183:805-816
608 Sun WD, Li SG, Chen YD, Li YJ (2002a) Timing of synorogenic granitoids in the South
609 Qinling, central China: constraints on the evolution of the Qinling–Dabie orogenic belt. J
610 Geol 110:457-468
611 Sun WD, Li SG, Sun Y, Zhang GW, Li Q (2002b) Mid-Paleozoic collision in the North Qinling:
612 Sm–Nd, Rb–Sr and $^{40}Ar/^{39}Ar$ ages and their tectonic implications. J Asian Earth Sci

613 21:69-76
614 Sun SS, McDonough WF (1989) Chemical and isotopic systematics of oceanic basalts:
615 implications for mantle composition and processes. In: Saunders AD, Norry MJ (eds),
616 Magmatism in the ocean basins. Geol Soc London Spec Publ 42:313-345
617 Vervoort JD, Patchett PJ, Blichert-Toft J, Albarède F (1999) Relationships between Lu-Hf and
618 Sm-Nd isotopic systems in the global sedimentary system. Earth Planet Sci Lett 168:79-
619 99
620 Vervoort JD, Plank T, Prytulak J (2011) The Hf-Nd isotopic composition of marine sediments.
621 Geochim Cosmochim Acta 75:5903-5926
622 Wall VJ, Clemens JD, Clarke DB (1987) Models for granitoid evolution and source
623 compositions. J Geol 95:731-749
624 Wang F, Lu XX, Lo CH, Wu FY, He HY, Yang LK, Zhu RX (2007) Post-collisional, potassic
625 monzonite–minette complex (Shahewan) in the Qinling Mountains (central China):
626 $^{40}Ar/^{39}Ar$ thermochronology, petrogenesis, and implications for the dynamic setting of the
627 Qinling orogen. J Asian Earth Sci 31:153-166
628 Wang XX, Wang T, Castro A, Pedreira R, Lu XX, Xiao QH (2011) Triassic granitoids of the
629 Qinling orogen, central China: genetic relationship of enclaves and rapakivi-textured
630 rocks. Lithos 2011:369-387
631 Wang XX, Wang T, Zhang CL (2015) Granitoid magmatism in the Qinling orogen, central
632 China and its bearing on orogenic evolution. Sci China Earth Sci 58:1497-1512
633 Wang YL, Zhang CQ, Wang CH, Hou KJ (2012) Hf isotopic composition of the Qinjia granites
634 from the Debao Cu deposit, Guangxi: Implications for crust - mantle interaction.
635 Geotectonica et Metallogenia 36:377-383
636 Wang ZQ, Yan QR, Yan Z, Wang T, Jiang CF, Gao LD, Liu P (2009) The new division of the
637 main tectonic unit for the Qinling orogenic belt. J Geol 83:1527-1546
638 Wei GJ, Liang XR, Li XH, Liu Y (2002) Precise measurement of Sr isotopic composition of
639 liquid and solid base using (LP) MC-ICPMS. Geochimica 31:295-305
640 Whalen JB (1985) Geochemistry of an Island-Arc Plutonic Suite: the Uasilau-Yau Yau
641 Intrusive Complex, New Britain, P.N.G. J Petrol 26:603-632

642 Wiedenbeck M, Alle P, Corfu F, et al. (1995) Three natural zircon standards for U‐Th‐Pb,
643 Lu‐Hf, trace element and REE analyses. Geostandards Newslett 19:1-23
644 Wu FY, Jahn BM, Wilde SA, Lo CH, Yui TF, Lin Q, Ge WC, Sun DY (2003) Highly
645 fractionated I-type granites in NE China: geochronology and petrogenesis. Lithos 66:241-
646 273
647 Wu YB, Zheng YF (2012) Tectonic evolution of a composite collision orogen: an overview on
648 the Qinling–Tongbai–Hong'an–Dabie–Sulu orogenic belt in central China. Gondwana Res
649 23:1402-1428
650 Xiao B, Li QG, Liu SW, Wang ZQ, Yang PT, Chen JL, Xu XY (2013) Highly fractionated Late
651 Triassic I-type granites and related molybdenum mineralization in the Qinling orogenic
652 belt: Geochemical and U–Pb–Hf and Re–Os isotope constraints. Ore Geol Rev 56:220-
653 233
654 Xing FM, Xu X (1996) AFC mixing model and origin of intrusive rocks from Tongling area.
655 Acta Petrologica et Mineralogica 15:10-15
656 Xu JF, Castillo PR, Li XH, Zhang BR, Han YW (2002) MORB-type rocks from the Paleo-
657 Tethyan Mian-Lueyang northern ophiolite in the Qinling mountains, central China:
658 Implications for the source of the low $^{206}Pb/^{204}Pb$ and high $^{143}Nd/^{144}Nd$ mantle component
659 in the Indian ocean. Earth Planet Sci Lett 198:323-337
660 Xu XY, Li T, Chen JL, Li P (2013) The granitoids magmatism and mineralization in west
661 section of the western Qinling, NW China. Northwest geology 5:76-82
662 Xu XY, Chen JL, Gao T, Li P, Li T (2014) Granitoid magmatism and tectonic evolution in
663 northern edge of the West Qinling terrance, NW China. Acta Petrol Sin 30:371-389 (in
664 Chinese with English abstract)
665 Yang JS, Wu FY, Wilde S, Liu X (2007) Petrogenesis of late Triassic granitoids and their
666 enclaves with implications for post-collisional lithospheric thinning of the Liaodong
667 Peninsula, North China Craton. Chem Geol 242:155-175
668 Yang PT, Liu SW, Li QG, Zhang F, Wang ZQ, Wang DS, Wang RT, Yan QR, Yan Z (2011) Ages
669 of the Laocheng granitoids and crustal growth in the South Qinling tectonic domain,
670 Central China: zircon U–Pb and Lu–Hf isotopic constraints. Acta Geol Sin Engl 85:854-

869

Yang PT, Liu SW, Li QG, Wang ZQ, Wang RT, Wang W (2012) Geochemistry and zircon U–Pb-Hf isotopic systematics of the Ningshan granitoid batholith, middle segment of the South Qinling belt, Central China: constraints on petrogenesis and geodynamic processes. J Asian Earth Sci 61:166-186

Zhang CL, Zhang GW, Yan YX, Wang Y (2005) Origin and dynamic significance of Guangtoushan granitic plutons to the north of Mianlue zone in southern Qinling. Acta Petrol Sin 21:711-720 (in Chinese with English abstract)

Zhang GW, Zhang BR, Yuan XC, Xiao QH (2001) Qinling orogen belt and continental geodynamics. Science Press, Beijing, pp 1–729 (in Chinese)

Zhang HF, Jin LL, Zhang L, Nigel H, Zhou L, Hu SH, Zhang BR (2007) Geochemical and Pb-Sr-Nd isotopic compositions of granitoids from western Qinling belt: Constraints on basement nature and tectonic affinity. Science in China Series D: Earth Sciences 50:184-196

Zeng Q, McCuaig TC, Hart CJ, Jourdan F, Muhling J, Bagas L (2012) Structural and geochronological studies on the Liba goldfield of the West Qinling Orogen, Central China. Miner Deposita 7:799-819

Zeng Q, Mccuaig TC, Tohver E, Bagas L, Lu Y (2014) Episodic Triassic magmatism in the western south Qinling orogen, central China, and its implications. Geol J 49:402–423

Zhu LM, Ding ZJ, Yao SZ, Zhang WG, Song SG, Qu WJ, Guo B, Li B (2009) Ore forming event and geodynamic setting of molybdenum deposit at Wenquan in Gansu Province, Western Qinling. Chinese Sci Bull 54:2309-2324

Zhu LM, Zhang GW, Chen YJ, Ding ZJ, Guo B, Wang F, Lee B (2011) Zircon U-Pb ages and geochemistry of the Wenquan Mo-bearing granitoids in West Qinling, China: Constraints on the geodynamic setting for the newly discovered Wenquan Mo deposit. Ore Geol Rev 39:46-62

Zhu LM, Zhang GW, Yang T, Wang F, Gong HJ (2013) Geochronology, petrogenesis and tectonic implications of the Zhongchuan granitic pluton in the Western Qinling metallogenic belt, China. Geol J 48:310-334

700 **Figure captions**

701 **Fig. 1**. ***(a)***, ***(b)*** Simplified geological map of the western Qinling Orogenic belt (modified
702 from Zhang et al. 2007). In ***(c)*** I = fine grained porphyritic tourmaline-bearing biotite
703 monzonitic granite; II = fine grained porphyritic biotite monzonitic granite; III = medium-fine
704 grained biotite monzonitic granite; IV = medium-fine grained granodiorite; V = medium
705 grained biotite monzonitic granite; VI = porphyritic biotite monzonitic granite; VII =
706 porphyritic monzonitic granite; and VIII = medium to fine grained biotite monzonitic granite.

707 **Fig. 2**. ***(a)*** Outcrop of Luchuba granitoid pluton with mafic magmatic enclaves (MMEs).
708 ***(b)*** Outcrop of Wuchaba granitoid pluton with MMEs.

709 **Fig. 3**. Photomicrographs of Luchuba and Wuchaba plutons. ***(a)*** Sample SEB12-01 and
710 ***(b)*** Sample YDB12-05 of Luchuba (cross-polarized light or XPL) pluton; ***(c)*** Sample DPC12-
711 01 and ***(d)*** Sample MK12-04 of Wuchaba (XPL) pluton. ***(e)*** showing the sharp contact of
712 MMEs with their host granodiorite, and MMEs are finer-grained than the host. ***(f)*** Sample
713 MK12-04 of Wuchaba (PPL) pluton. The abbreviations are as follows: Pl - plagioclase, Qz -
714 quartz, Bt - biotite, Hb - hornblende, Kfs - K-feldspar, Ap - apatite, Zr - zircon.

715 **Fig. 4**. Cathodoluminescence (CL) images of zircons from representative samples ***(a)***
716 SEB12-01 and ***(b)*** YDB12-05 of Luchuba pluton; ***(c)*** DPC12-01 of Wuchaba pluton. Red
717 circles show analyzed spots.

718 **Fig. 5**. Zircon U–Pb concordia plots and weighted mean $^{206}Pb/^{238}U$ ages for ***(a)*** SEB12-
719 01 and ***(b)*** YDB12-05 of Luchuba pluton, and ***(c)*** DPC12-01 of Wuchaba pluton.

720 **Fig. 6**. Total alkalis ($Na_2O + K_2O$) versus SiO_2 (TAS) diagram showing the compositional
721 variation of Luchuba and Wuchaba samples. The MMEs are less felsic than the hosts.

722 **Fig. 7**. Diagram of A/NK [$Al_2O_3/(Na_2O + K_2O)$] vs. A/CNK [molar ratio $Al_2O_3/(CaO + Na_2O$
723 $+ K_2O)$] for granitoids of Luchuba and Wuchaba plutons in WQOB.

724 **Fig. 8**. SiO_2 variation diagrams of representative major elements (wt.%) and selected trace
725 elements (ppm) of Luchuba and Wuchaba samples.

726 **Fig. 9**. ***(a)*** Chondrite normalized REE patterns, and ***(b)*** Primitive mantle normalized
727 incompatible element patterns of samples from Luchuba pluton; ***(c)*** Chondrite normalized REE
728 patterns, and ***(d)*** Primitive mantle normalized incompatible element patterns of samples from
729 Wuchaba pluton. For comparison, the average bulk continental crust (BCC, red solid line)
730 (Rudnick and Gao 2003) is also plotted. Chondrite and primitive mantle values are from Sun
731 and McDonough (1989).

732 **Fig. 10**. Plot of Sr/Sr* vs. Eu/Eu* for the Luchuba and Wuchaba granitoids. $Sr/Sr^* = Sr_{PM}/[1/2*(Pr_{PM} \times Nd_{PM})]$; $Eu/Eu^* = Eu_{PM}/[1/2*(Sm_{PM} \times Gd_{PM})]$; Primitive mantle values are
734 from Sun and McDonough (1989).

735 **Fig. 11**. ***(a)*** Plot of I_{Sr} vs. 1/Sr for the Luchuba and Wuchaba granitoids. ***(b)*** Plot of $\varepsilon_{Nd}(t)$
736 vs. 1/Nd for the Luchuba and Wuchaba granitoids.

737 **Fig. 12**. Plots of Sr, Nd and Hf isotopes (in the forms of initial $^{87}Sr/^{86}Sr$ or I_{Sr}, $\varepsilon_{Nd}(t)$ and
738 $\varepsilon_{Hf}(t)$) against MgO and SiO_2.

739 **Fig. 13**. ***(a)*** $\varepsilon_{Nd}(t)$ vs. I_{Sr} plot of the Luchuba and Wuchaba granitoids (modified after Qin
740 et al. 2009); the data for the Triassic granites in western Qinling are from Zhang et al. (2007).
741 ***(b)*** $\varepsilon_{Nd}(t)$ vs. $\varepsilon_{Hf}(t)$ plot. The field for crust-mantle array is from Vervoort et al. (1999) and the
742 terrestrial array is from Vervoort et al. (2011). ***(c)*** Age (Ma) vs. $\varepsilon_{Hf}(t)$ plot of the Luchuba and
743 Wuchaba granitoids, together with the literature Hf isotope data (Zhu et al. 2013).

744 **Fig. 14**. Plot of $\varepsilon_{Nd}(t)$ vs. $\varepsilon_{Hf}(t)$ for Luchuba and Wuchaba granitoids. The modeled AFC
745 path uses parental magma (Mianlue MORB) with 6.5 ppm Nd ($\varepsilon_{Nd}(t)$: 8.71) and 1.87 ppm Hf
746 ($\varepsilon_{Hf}(t)$: 16.7) (Xu et al. 2002) and a mature continental crust with 26 ppm Nd ($\varepsilon_{Nd}(t)$: -14.5) and
747 5.8 ppm Hf ($\varepsilon_{Hf}(t)$: -16.8) (Shen et al. 1997) for conceptual simplicity. The Hf isotope
748 composition for MORB is inferred from Nd isotope according to the equation ($\varepsilon_{Hf} = 1.59\varepsilon_{Nd} +$
749 1.28) given by (Chauvel et al. 2008), for continental crust according to the equation ($\varepsilon_{Hf} =$
750 $1.36\varepsilon_{Nd} + 2.95$) given by (Vervoort et al. 1999). AFC path calculated according to (DePaolo et
751 al. 1981) equation. The ratio of assimilation to fractionation was set at r = 0.5. Bulk Kd's for
752 Nd and Hf were 0.4 and 0.6, respectively. The partition coefficients of Nd and Hf for amphibole
753 and plagioclase are from Bacon and Druitt (1988) and for biotite from Schnetzler and Philpotts
754 (1970) and Higuchi and Nagasawa (1969).

755 **Fig. 15**. Proposed tectonic model for the generation of the Luchuba and Wuchaba
756 granitoids in West Qinling during the late Triassic (~220Ma). See text for explanation.

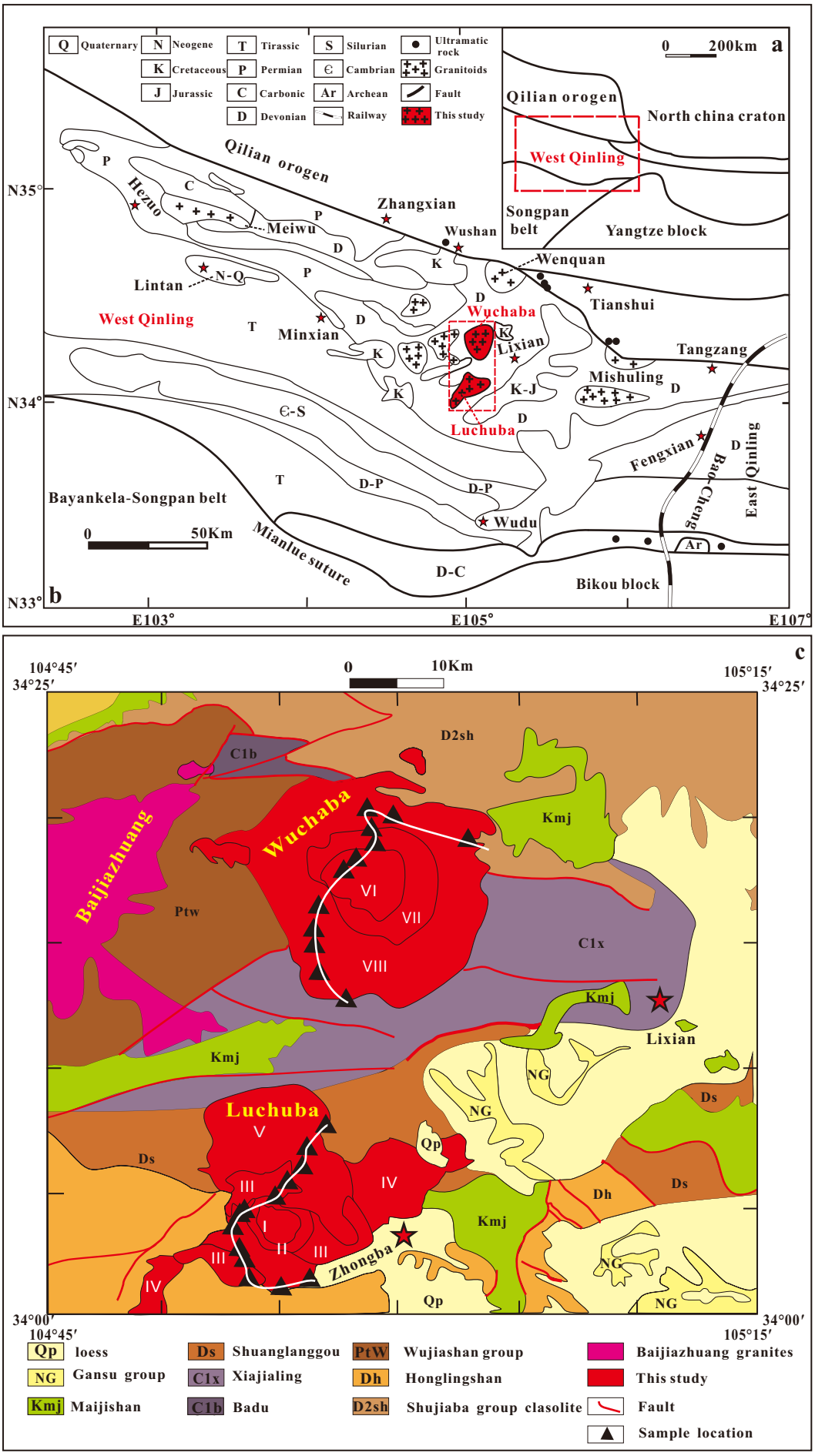
a
0 200km
Qilian orogen
North china craton
West Qinling
Songpan belt
Yangtze block
b
Q Quaternary
N Neogene
K Cretaceous
J Jurassic
T Tirassic
P Permian
C Carbonic
D Devonian
S Silurian
Cambrian
Ar Archean
Railway
Ultramatic rock
Granitoids
Fault
This study
Qilian orogen
Hezuo
Meiwu
Zhangxian
Wushan
Wenquan
Tianshui
Lintan
N-Q
West Qinling
Minxian
Wuchaba
Lixian
Tangzang
Mishuling
K-J
Luchuba
Fengxian
Bao-Chen
East Qinling
Bayankela-Songpan belt
Mianlue suture
Wudu
Bikou block
0 50Km
N35°
N34°
N33°
E103°
E105°
E107°
c
104°45′
34°25′
0 10Km
105°15′
34°25′
D2sh
C1b
Baijiazhuang
Wuchaba
Kmj
Ptw
C1x
VI
VII
VIII
Lixian
NG
Ds
Luchuba
V
Qp
Dh
III
IV
I
II
Zhongba
34°00′
104°45′
105°15′
34°00′
Qp loess
NG Gansu group
Kmj Maijishan
Ds Shuanglanggou
C1x Xiajialing
C1b Badu
PtW Wujiashan group
Dh Honglingshan
D2sh Shujiaba group clasolite
Baijiazhuang granites
This study
Fault
Sample location

Fig.1

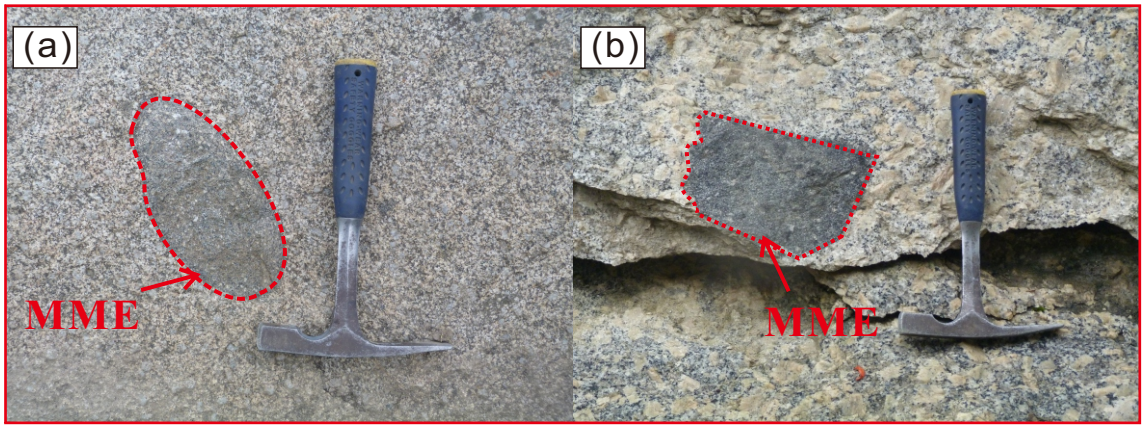
(a)
MME
(b)
MME

Fig.2

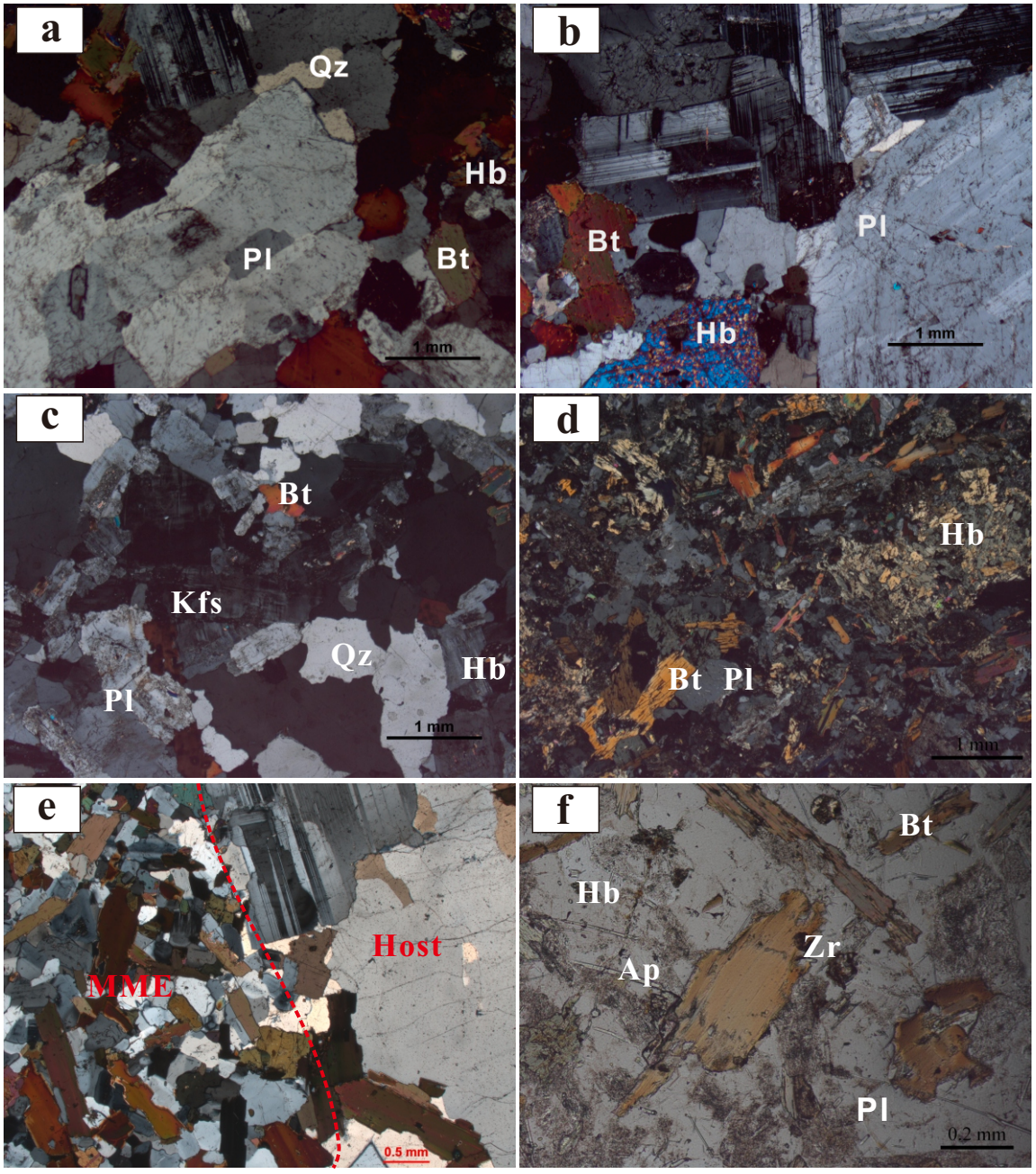
a
Qz
Hb
Pl
Bt
1 mm
b
Bt
Pl
Hb
1 mm
c
Bt
Kfs
Qz
Hb
Pl
1 mm
d
Hb
Bt Pl
1 mm
e
Host
MME
0.5 mm
f
Bt
Hb
Zr
Ap
Pl
0.2 mm

Fig.3

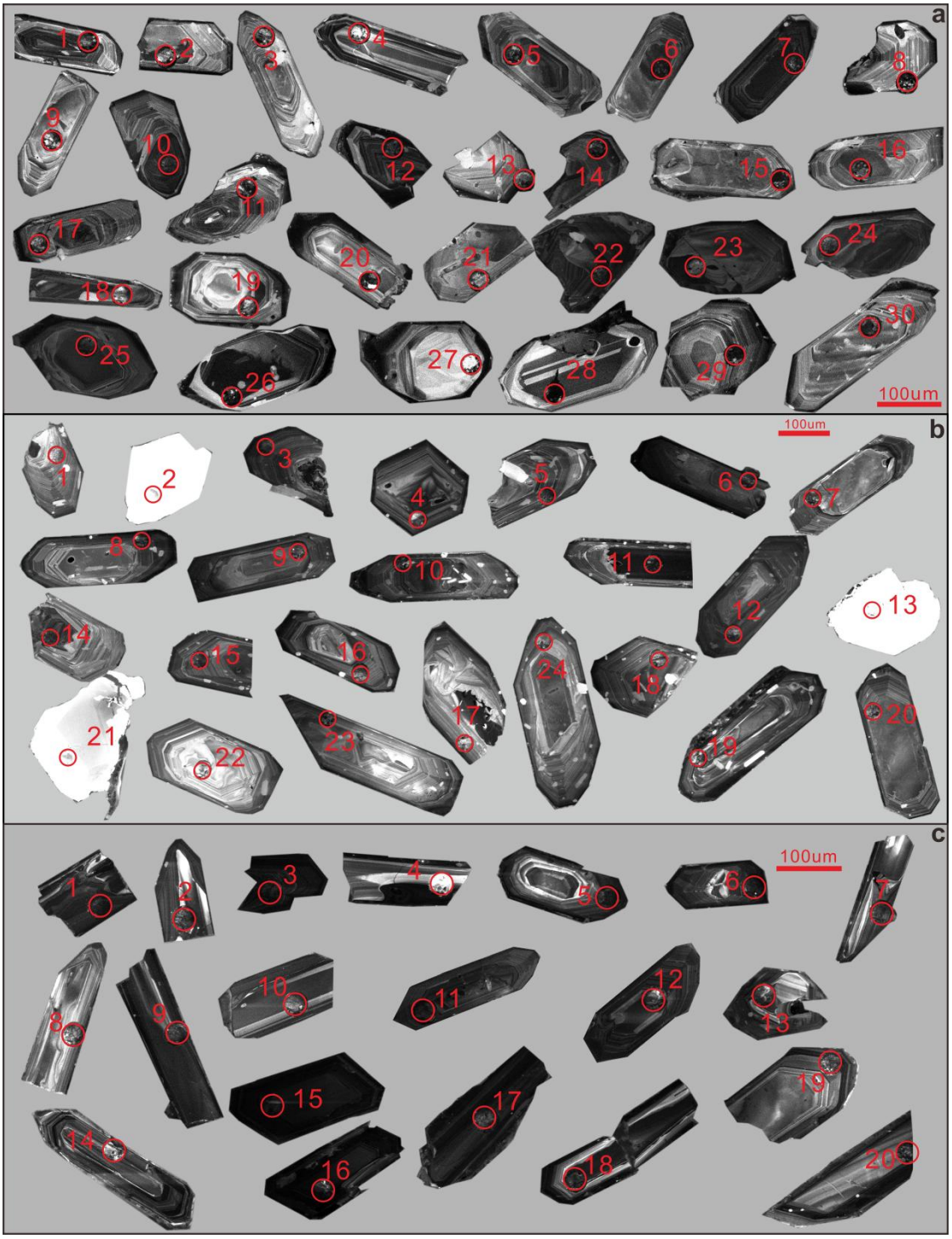

Fig.4

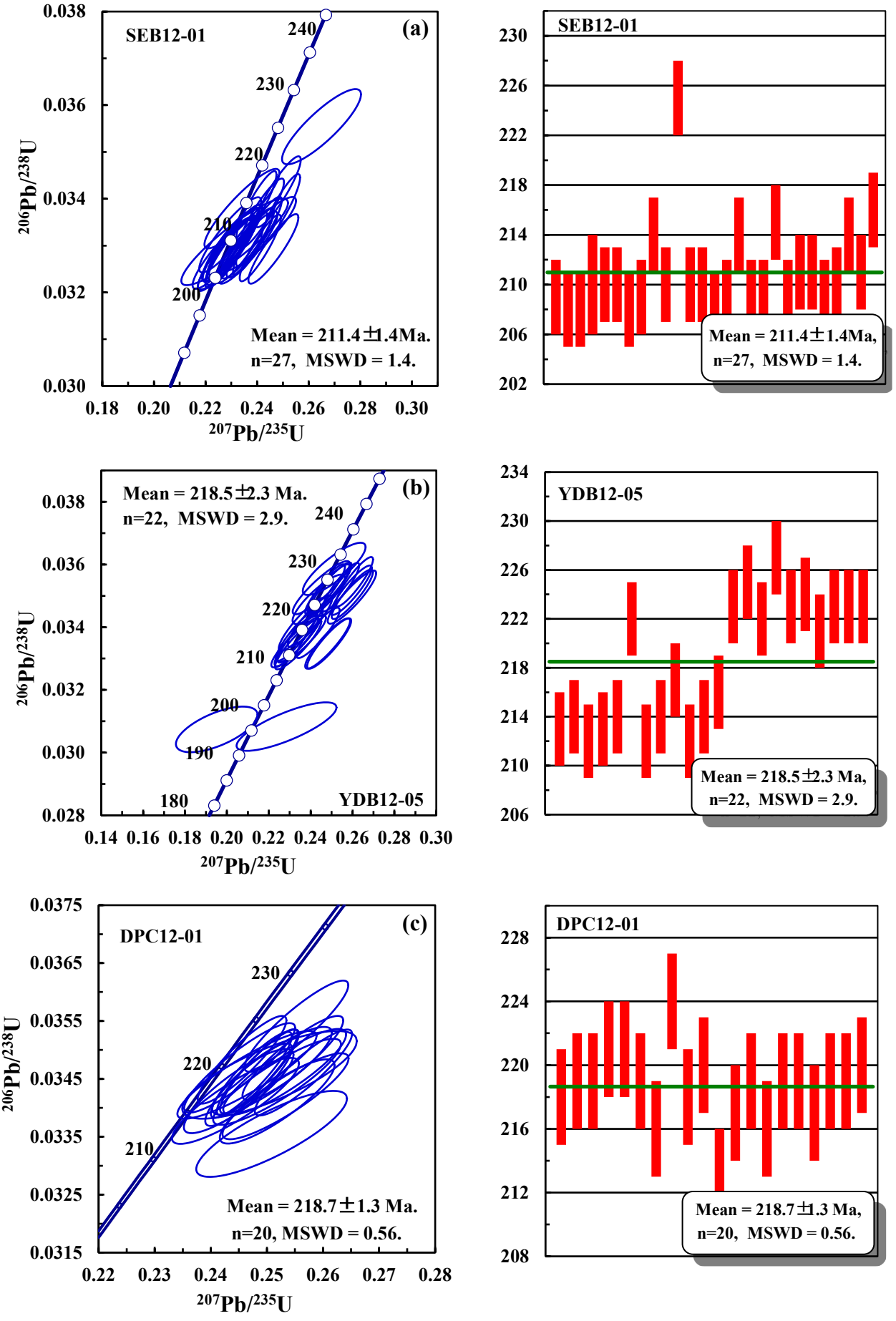
SEB12-01
(a)
240
230
220
210
200
Mean = 211.4±1.4Ma.
n=27, MSWD = 1.4.
$^{206}Pb/^{238}U$
$^{207}Pb/^{235}U$
SEB12-01
Mean = 211.4±1.4Ma,
n=27, MSWD = 1.4.
Mean = 218.5±2.3 Ma.
n=22, MSWD = 2.9.
(b)
240
230
220
210
200
190
180
YDB12-05
YDB12-05
Mean = 218.5±2.3 Ma,
n=22, MSWD = 2.9.
DPC12-01
(c)
230
220
210
Mean = 218.7±1.3 Ma.
n=20, MSWD = 0.56.
DPC12-01
Mean = 218.7±1.3 Ma,
n=20, MSWD = 0.56.

Fig.5

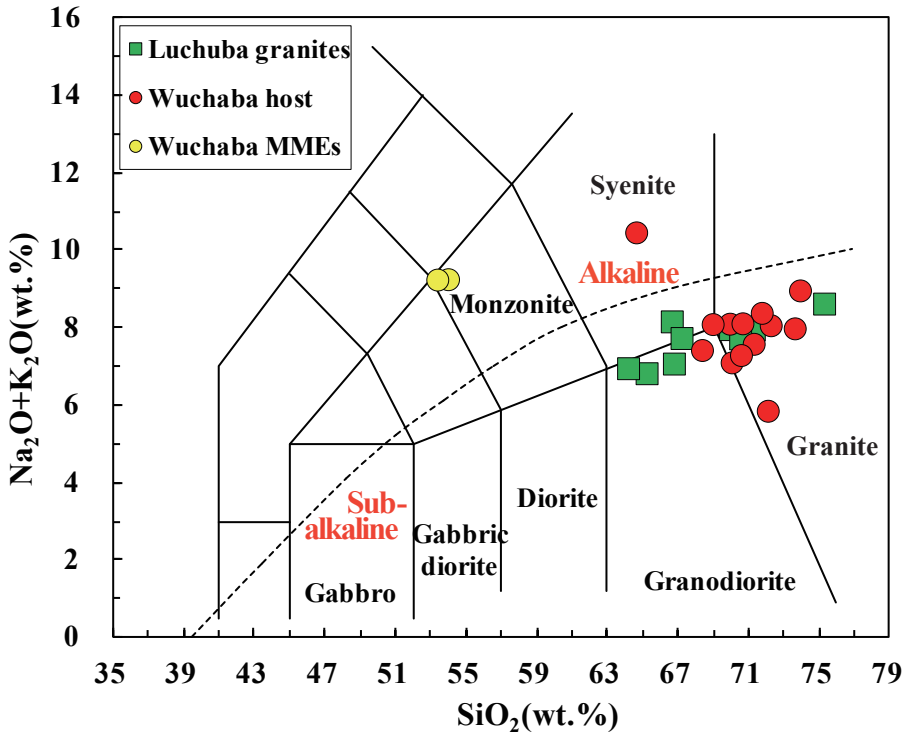
Luchuba granites
Wuchaba host
Wuchaba MMEs
Syenite
Alkaline
Monzonite
Granite
Diorite
Sub-
alkaline
Gabbric
diorite
Gabbro
Granodiorite
Na2O+K2O(wt.%)
SiO2(wt.%)
0
2
4
6
8
10
12
14
16
35
39
43
47
51
55
59
63
67
71
75
79

Fig.6

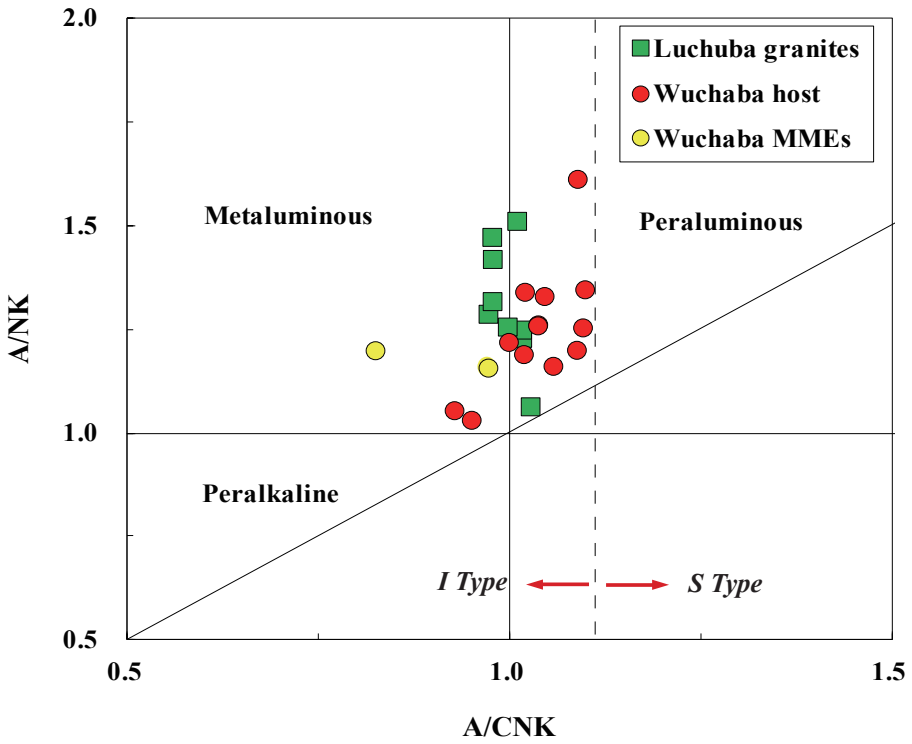
2.0
1.5
1.0
0.5
A/NK
Luchuba granites
Wuchaba host
Wuchaba MMEs
Metaluminous
Peraluminous
Peralkaline
I Type
S Type
0.5
1.0
1.5
A/CNK

Fig.7

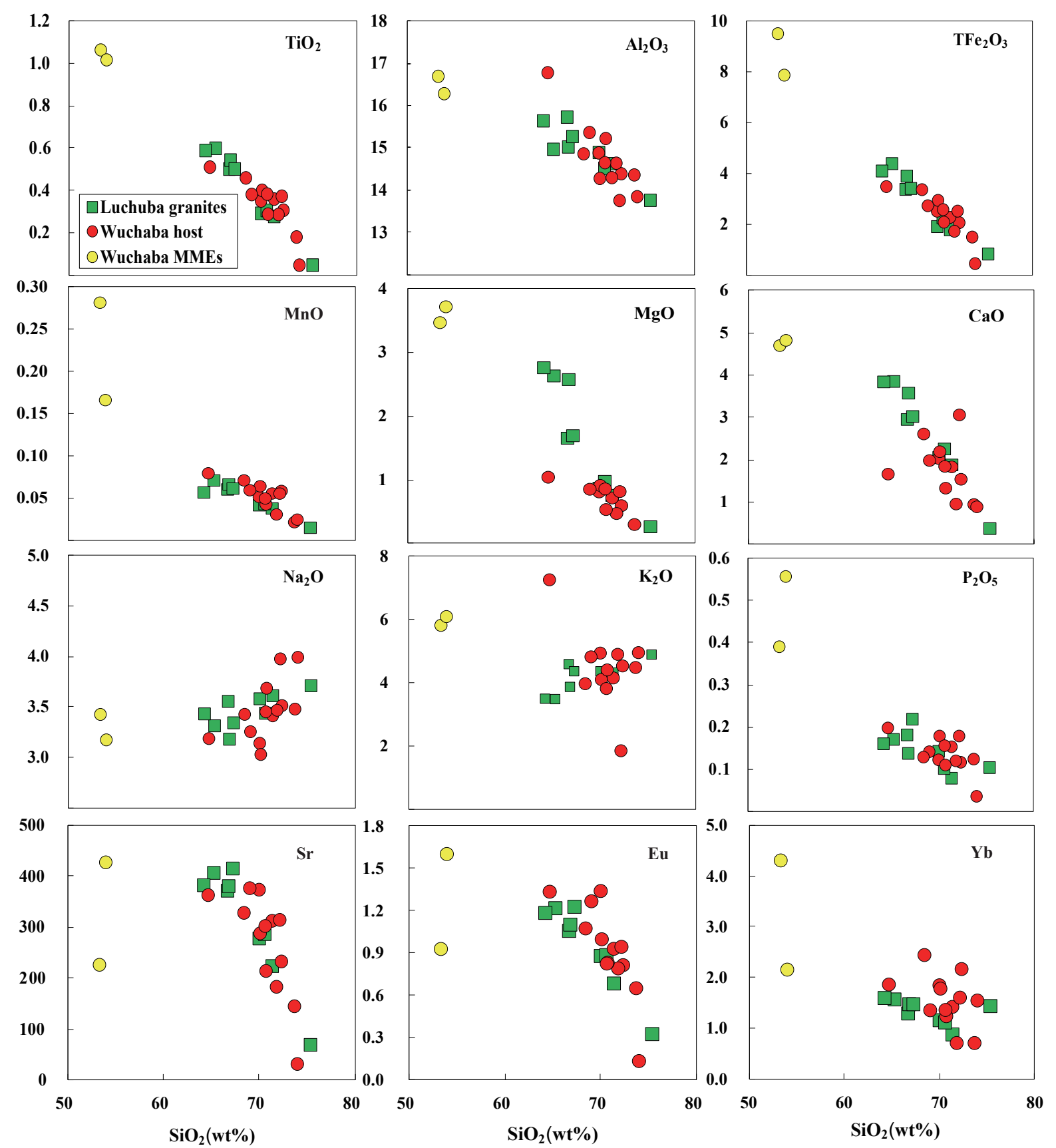
TiO2
Al2O3
TFe2O3
MnO
MgO
CaO
Na2O
K2O
P2O5
Sr
Eu
Yb
Luchuba granites
Wuchaba host
Wuchaba MMEs
SiO2(wt%)
SiO2(wt%)
SiO2(wt%)

Fig.8

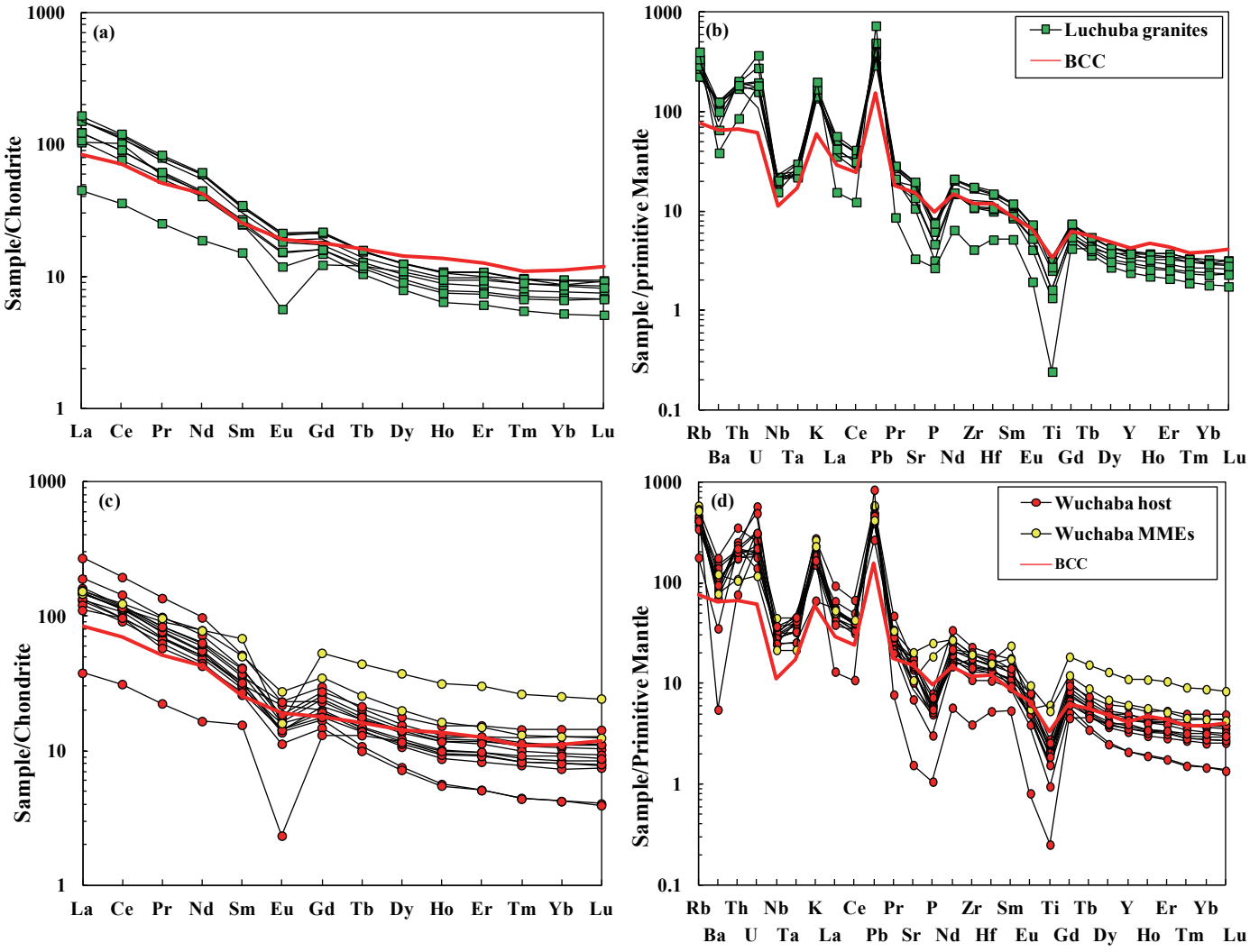
(a)
Sample/Chondrite
1000
100
10
1
La Ce Pr Nd Sm Eu Gd Tb Dy Ho Er Tm Yb Lu
(b)
Luchuba granites
BCC
Sample/primitive Mantle
0.1
Rb Th Nb K Ce Pr P Zr Sm Ti Tb Y Er Yb
Ba U Ta La Pb Sr Nd Hf Eu Gd Dy Ho Tm Lu
(c)
(d)
Wuchaba host
Wuchaba MMEs
BCC
Sample/Primitive Mantle

Fig.9

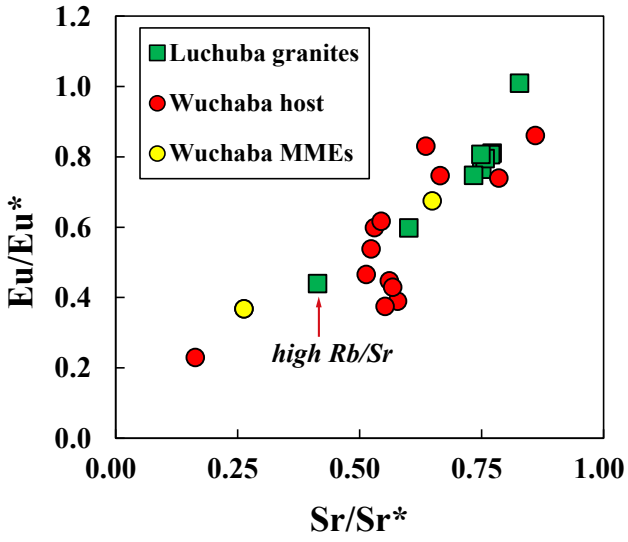
Luchuba granites
Wuchaba host
Wuchaba MMEs
high Rb/Sr
Eu/Eu*
Sr/Sr*
1.2
1.0
0.8
0.6
0.4
0.2
0.0
0.00
0.25
0.50
0.75
1.00

Fig.10

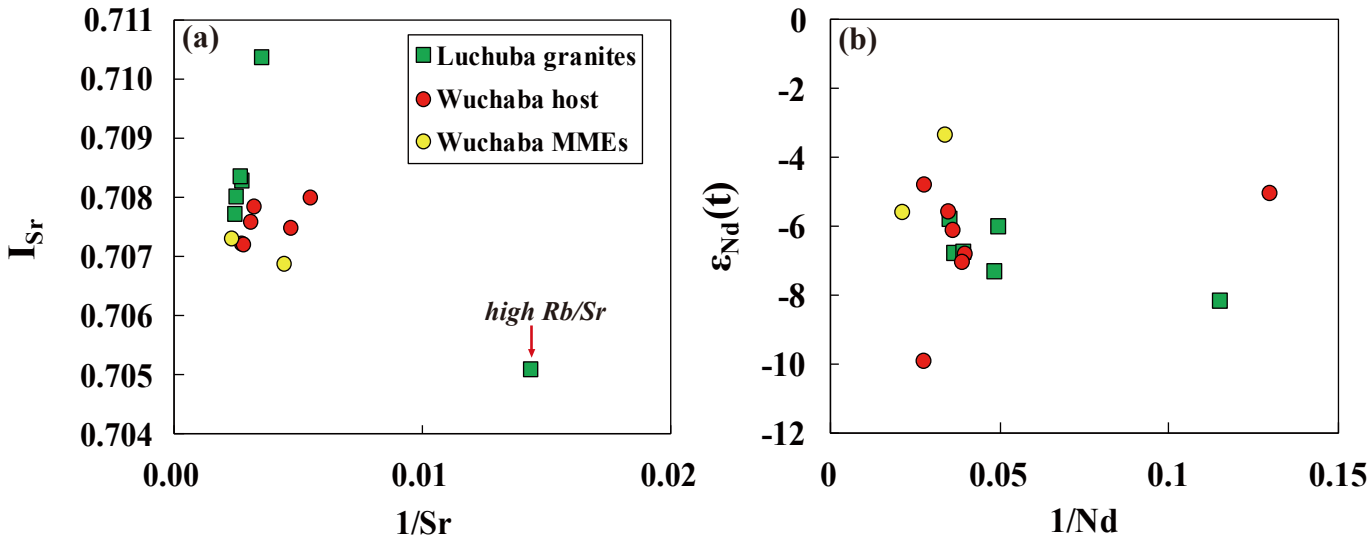
(a)
Luchuba granites
Wuchaba host
Wuchaba MMEs
high Rb/Sr
I_{Sr}
1/Sr
0.711
0.710
0.709
0.708
0.707
0.706
0.705
0.704
0.00
0.01
0.02
(b)
$\varepsilon_{Nd}(t)$
1/Nd
0
-2
-4
-6
-8
-10
-12
0
0.05
0.1
0.15

Fig.11

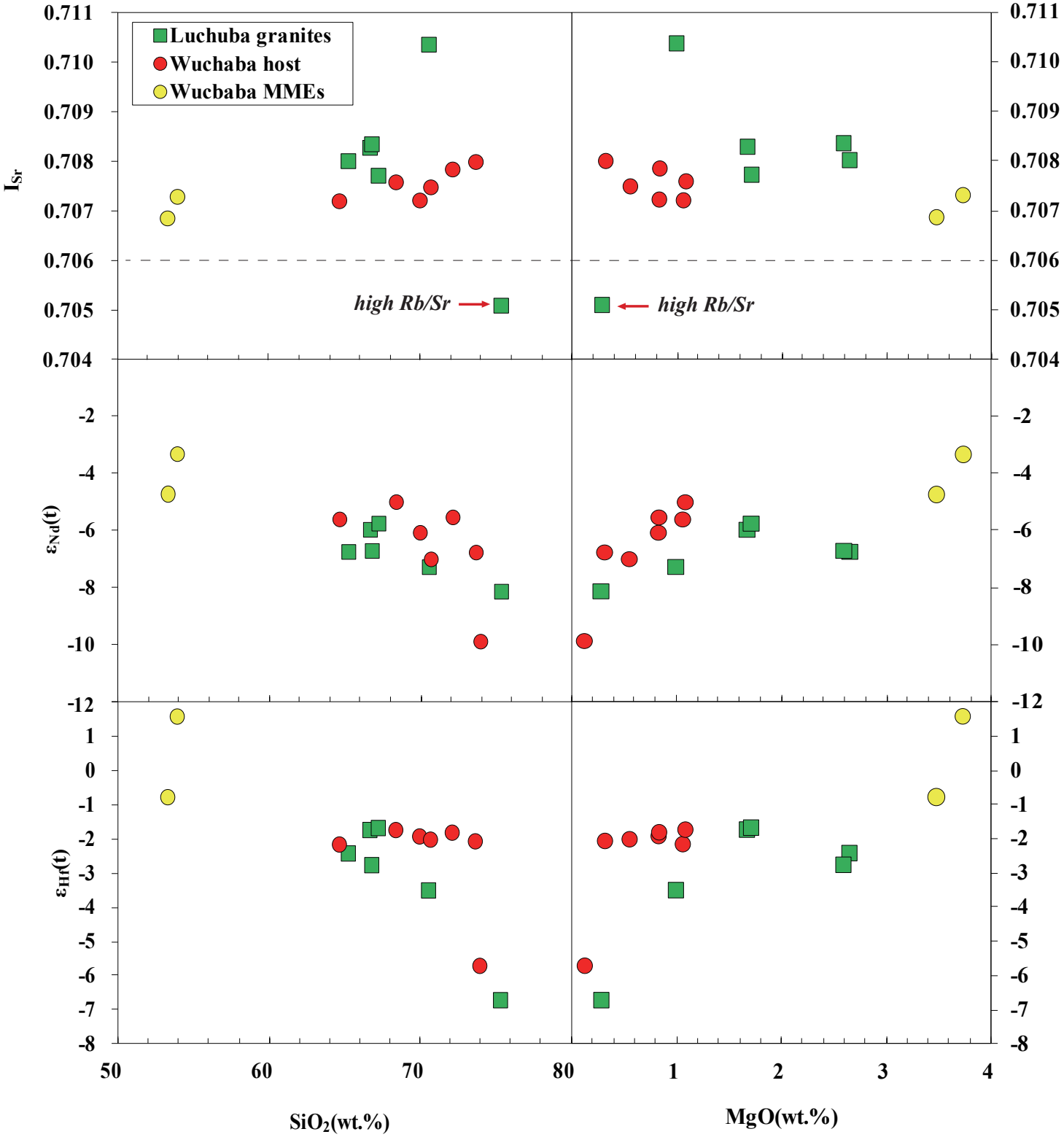
Luchuba granites
Wuchaba host
Wucbaba MMEs
high Rb/Sr
high Rb/Sr
I_{Sr}
$\varepsilon_{Nd}(t)$
$\varepsilon_{Hf}(t)$
SiO_2(wt.%)
MgO(wt.%)

Fig.12

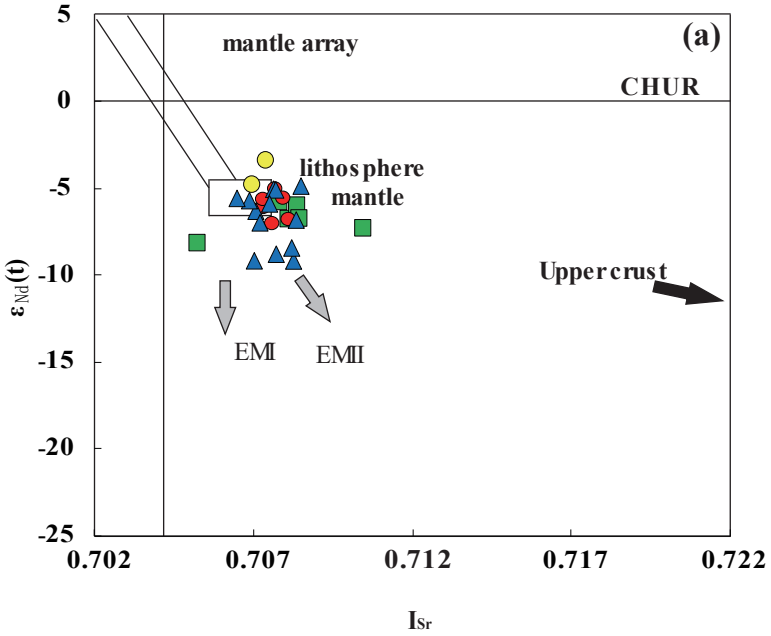
(a)
mantle array
CHUR
lithosphere mantle
Upper crust
EMI
EMII
$\varepsilon_{Nd}(t)$
I_{Sr}
5
0
-5
-10
-15
-20
-25
0.702
0.707
0.712
0.717
0.722

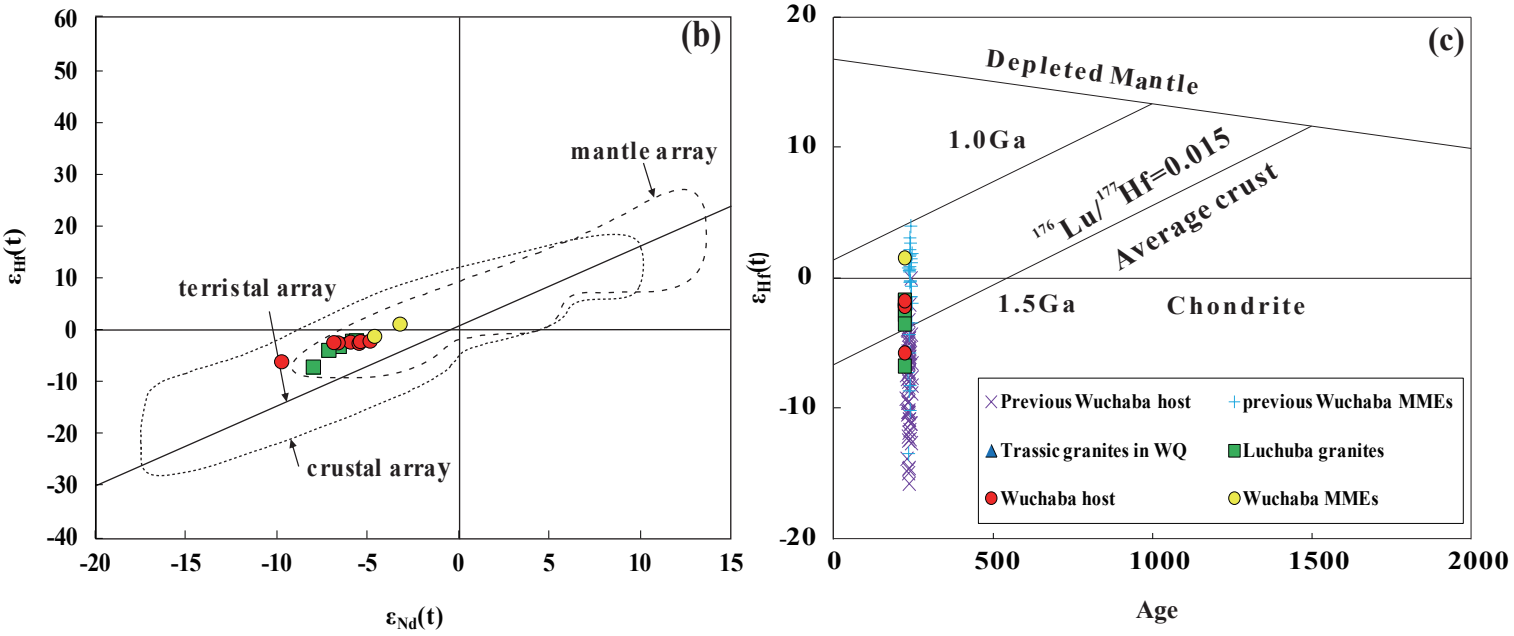
(b)
mantle array
terristal array
crustal array
$\varepsilon_{Hf}(t)$
$\varepsilon_{Nd}(t)$
(c)
Depleted Mantle
1.0Ga
$^{176}Lu/^{177}Hf$=0.015
Average crust
1.5Ga
Chondrite
Previous Wuchaba host
previous Wuchaba MMEs
Trassic granites in WQ
Luchuba granites
Wuchaba host
Wuchaba MMEs
$\varepsilon_{Hf}(t)$
Age

Fig.13

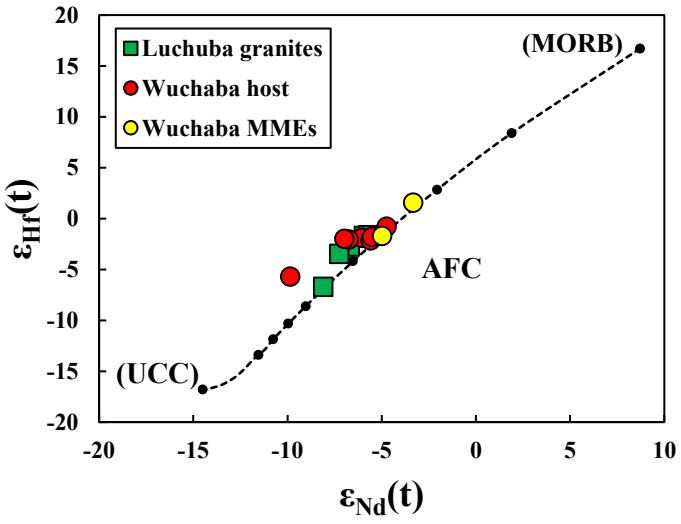
Luchuba granites
Wuchaba host
Wuchaba MMEs
(MORB)
AFC
(UCC)
$\varepsilon_{Hf}(t)$
$\varepsilon_{Nd}(t)$
20
15
10
5
0
-5
-10
-15
-20
-20
-15
-10
-5
0
5
10

Fig.14

~Late Trassic (220Ma)

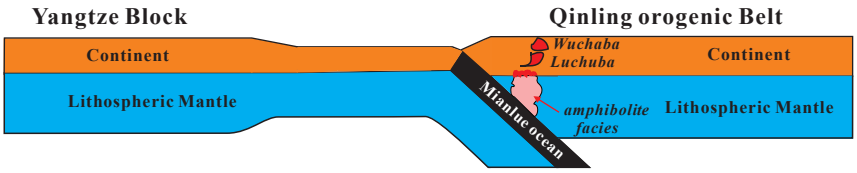

Fig.15

Table 1 Zircon U–Pb data for the Luchuba and Wuchaba pluton.

No.	Element（ppm）			Th/U	Isotope ratio						Apparent age(Ma)					
	Pb*	U	Th		$^{207}Pb/^{206}Pb$	1	$^{207}Pb/^{235}U$	1	$^{206}Pb/^{238}U$	1	$^{207}Pb/^{206}Pb$	1	$^{207}Pb/^{235}U$	1	$^{206}Pb/^{238}U$	1
Sample SEB12-01(Luchuba Pluton)																
SEB-1	19.7	559	261	0.47	0.0543	0.0014	0.2463	0.0064	0.0329	0.0005	381	32	224	5	209	3
SEB-2	16.1	459	183	0.40	0.0505	0.0016	0.2284	0.0074	0.0328	0.0005	216	47	209	6	208	3
SEB-3	16.4	441	269	0.61	0.0502	0.0018	0.2273	0.0081	0.0329	0.0005	202	54	208	7	208	3
SEB-4	6.4	175	105	0.60	0.0507	0.0030	0.2313	0.0137	0.0331	0.0006	227	102	211	11	210	4
SEB-5	18.1	517	174	0.34	0.0507	0.0014	0.2315	0.0068	0.0331	0.0005	227	40	211	6	210	3
SEB-6	21.7	568	400	0.70	0.0518	0.0014	0.2361	0.0067	0.0330	0.0005	277	38	215	5	210	3
SEB-7	18.5	525	211	0.40	0.0503	0.0015	0.2273	0.0068	0.0328	0.0005	208	42	208	6	208	3
SEB-8	18.8	511	285	0.56	0.0507	0.0014	0.2299	0.0066	0.0329	0.0005	226	39	210	5	209	3
SEB-9	31.4	914	191	0.21	0.0520	0.0012	0.2418	0.0057	0.0337	0.0005	287	29	220	5	214	3
SEB-10	13.9	389	164	0.42	0.0587	0.0019	0.2674	0.0086	0.0330	0.0005	557	44	241	7	209	3
SEB-11	18.0	223	182	0.81	0.0547	0.0017	0.5114	0.0159	0.0677	0.0010	402	43	419	11	423	6
SEB-12	15.7	445	164	0.37	0.0506	0.0014	0.2307	0.0067	0.0331	0.0005	224	40	211	6	210	3
SEB-13	28.2	796	298	0.37	0.0523	0.0011	0.2385	0.0052	0.0331	0.0005	297	25	217	4	210	3
SEB-14	19.1	486	149	0.31	0.0541	0.0022	0.2650	0.0101	0.0355	0.0005	374	95	239	8	225	3
SEB-15	15.7	446	154	0.35	0.0508	0.0015	0.2318	0.0069	0.0331	0.0005	230	41	212	6	210	3
SEB-16	20.0	571	215	0.38	0.0507	0.0014	0.2295	0.0063	0.0328	0.0005	226	37	210	5	208	3
SEB-17	21.6	624	189	0.30	0.0515	0.0014	0.2340	0.0066	0.0330	0.0005	262	38	213	5	209	3
SEB-18	56.7	1655	281	0.17	0.0535	0.0010	0.2491	0.0050	0.0338	0.0005	348	22	226	4	214	3
SEB-19	36.4	1087	250	0.23	0.0531	0.0011	0.2412	0.0053	0.0330	0.0005	333	25	219	4	209	3
SEB-20	24.9	728	190	0.26	0.0502	0.0014	0.2283	0.0064	0.0330	0.0005	204	38	209	5	209	3
SEB-21	46.5	1336	306	0.23	0.0514	0.0010	0.2397	0.0051	0.0339	0.0005	257	25	218	4	215	3

(continued)

SEB-22	**22.8**	**625**	**336**	**0.54**	**0.0503**	**0.0014**	**0.2288**	**0.0065**	**0.0330**	**0.0005**	**209**	**39**	**209**	**5**	**209**	**3**
SEB-23	**15.1**	**423**	**172**	**0.41**	**0.0525**	**0.0021**	**0.2408**	**0.0095**	**0.0333**	**0.0005**	**308**	**61**	**219**	**8**	**211**	**3**
SEB-24	**42.1**	**1219**	**301**	**0.25**	**0.0524**	**0.0012**	**0.2407**	**0.0058**	**0.0333**	**0.0005**	**304**	**30**	**219**	**5**	**211**	**3**
SEB-25	**21.2**	**597**	**224**	**0.38**	**0.0520**	**0.0016**	**0.2365**	**0.0075**	**0.0330**	**0.0005**	**286**	**45**	**216**	**6**	**209**	**3**
SEB-26	**29.4**	**867**	**186**	**0.21**	**0.0521**	**0.0013**	**0.2374**	**0.0061**	**0.0331**	**0.0005**	**288**	**32**	**216**	**5**	**210**	**3**
SEB-27	**12.5**	**360**	**77**	**0.21**	**0.0502**	**0.0021**	**0.2341**	**0.0096**	**0.0338**	**0.0006**	**206**	**64**	**214**	**8**	**214**	**3**
SEB-28	**15.4**	**419**	**135**	**0.32**	**0.0501**	**0.0017**	**0.2296**	**0.0079**	**0.0332**	**0.0005**	**200**	**51**	**210**	**7**	**211**	**3**
SEB-29	**24.3**	**525**	**435**	**0.83**	**0.0980**	**0.0043**	**0.4712**	**0.0192**	**0.0349**	**0.0006**	**1586**	**84**	**392**	**13**	**221**	**4**
SEB-30	**37.1**	**1061**	**232**	**0.22**	**0.0527**	**0.0012**	**0.2481**	**0.0058**	**0.0342**	**0.0005**	**315**	**28**	**225**	**5**	**216**	**3**
Sample YDB12-05(Luchuba pluton)																
YDB-1	**24.8**	**719**	**136**	**0.19**	**0.0504**	**0.0015**	**0.2332**	**0.0069**	**0.0336**	**0.0005**	**213**	**40**	**213**	**6**	**213**	**3**
YDB-2	**31.8**	**897**	**223**	**0.25**	**0.0522**	**0.0015**	**0.2435**	**0.0068**	**0.0338**	**0.0005**	**295**	**36**	**221**	**6**	**214**	**3**
YDB-3	**29.1**	**836**	**186**	**0.22**	**0.0537**	**0.0015**	**0.2481**	**0.0071**	**0.0335**	**0.0005**	**360**	**37**	**225**	**6**	**212**	**3**
YDB-4	**12.4**	**353**	**84**	**0.24**	**0.0506**	**0.0019**	**0.2343**	**0.0086**	**0.0336**	**0.0006**	**224**	**55**	**214**	**7**	**213**	**3**
YDB-5	**25.7**	**725**	**198**	**0.27**	**0.0506**	**0.0015**	**0.2350**	**0.0071**	**0.0337**	**0.0005**	**220**	**41**	**214**	**6**	**214**	**3**
YDB-6	**29.6**	**800**	**212**	**0.27**	**0.0539**	**0.0016**	**0.2597**	**0.0076**	**0.0350**	**0.0006**	**366**	**38**	**234**	**6**	**222**	**3**
YDB-7	**26.2**	**747**	**185**	**0.25**	**0.0539**	**0.0015**	**0.2489**	**0.0069**	**0.0335**	**0.0005**	**366**	**35**	**226**	**6**	**212**	**3**
YDB-8	**31.1**	**879**	**207**	**0.24**	**0.0506**	**0.0015**	**0.2349**	**0.0070**	**0.0337**	**0.0005**	**220**	**40**	**214**	**6**	**214**	**3**
YDB-9	**31.4**	**771**	**159**	**0.21**	**0.0538**	**0.0038**	**0.2285**	**0.0158**	**0.0308**	**0.0005**	**360**	**164**	**209**	**13**	**196**	**3**
YDB-10	**28.4**	**787**	**209**	**0.27**	**0.0508**	**0.0015**	**0.2397**	**0.0070**	**0.0342**	**0.0005**	**233**	**39**	**218**	**6**	**217**	**3**
YDB-11	**27.3**	**782**	**187**	**0.24**	**0.0507**	**0.0016**	**0.2341**	**0.0073**	**0.0335**	**0.0005**	**228**	**43**	**214**	**6**	**212**	**3**
YDB-12	**45.7**	**1315**	**257**	**0.20**	**0.0502**	**0.0014**	**0.2334**	**0.0066**	**0.0337**	**0.0005**	**202**	**37**	**213**	**5**	**214**	**3**
YDB-13	**26.9**	**751**	**195**	**0.26**	**0.0502**	**0.0016**	**0.2360**	**0.0074**	**0.0341**	**0.0006**	**204**	**43**	**215**	**6**	**216**	**3**
YDB-14	**22.0**	**596**	**189**	**0.32**	**0.0504**	**0.0018**	**0.2451**	**0.0090**	**0.0353**	**0.0006**	**213**	**56**	**223**	**7**	**223**	**3**
YDB-15	**63.9**	**1718**	**805**	**0.47**	**0.0534**	**0.0011**	**0.2609**	**0.0059**	**0.0355**	**0.0005**	**344**	**26**	**235**	**5**	**225**	**3**

(continued)

YDB-16	**36.9**	**1009**	**266**	**0.26**	**0.0538**	**0.0013**	**0.2599**	**0.0065**	**0.0351**	**0.0005**	**361**	**31**	**235**	**5**	**222**	**3**
YDB-17	**22.1**	**586**	**136**	**0.23**	**0.0508**	**0.0022**	**0.2513**	**0.0099**	**0.0359**	**0.0006**	**233**	**100**	**228**	**8**	**227**	**3**
YDB-18	**29.5**	**805**	**215**	**0.27**	**0.0511**	**0.0014**	**0.2481**	**0.0071**	**0.0352**	**0.0005**	**245**	**38**	**225**	**6**	**223**	**3**
YDB-19	**42.7**	**883**	**240**	**0.27**	**0.0461**	**0.0031**	**0.1952**	**0.0129**	**0.0307**	**0.0005**		**149**	**181**	**11**	**195**	**3**
YDB-20	**39.7**	**1105**	**229**	**0.21**	**0.0523**	**0.0011**	**0.2543**	**0.0059**	**0.0353**	**0.0005**	**298**	**28**	**230**	**5**	**224**	**3**
YDB-21	**33.4**	**915**	**209**	**0.23**	**0.0507**	**0.0019**	**0.2439**	**0.0083**	**0.0349**	**0.0005**	**227**	**88**	**222**	**7**	**221**	**3**
YDB-22	**31.4**	**842**	**305**	**0.36**	**0.0535**	**0.0013**	**0.2594**	**0.0065**	**0.0352**	**0.0005**	**349**	**31**	**234**	**5**	**223**	**3**
YDB-23	**30.5**	**844**	**193**	**0.23**	**0.0510**	**0.0012**	**0.2474**	**0.0059**	**0.0352**	**0.0005**	**239**	**29**	**224**	**5**	**223**	**3**
YDB-24	**19.4**	**523**	**157**	**0.30**	**0.0513**	**0.0013**	**0.2495**	**0.0067**	**0.0353**	**0.0005**	**255**	**35**	**226**	**5**	**223**	**3**
Sample DPC12-01(Wuchaba pluton)																
DPC-1	**80.6**	**2330**	**169**	**0.07**	**0.0520**	**0.0013**	**0.2467**	**0.0051**	**0.0344**	**0.0005**	**286**	**58**	**224**	**4**	**218**	**3**
DPC-2	**37.8**	**998**	**424**	**0.43**	**0.0517**	**0.0019**	**0.2465**	**0.0082**	**0.0346**	**0.0005**	**272**	**85**	**224**	**7**	**219**	**3**
DPC-3	**43.7**	**1251**	**208**	**0.17**	**0.0519**	**0.0009**	**0.2472**	**0.0048**	**0.0346**	**0.0005**	**279**	**21**	**224**	**4**	**219**	**3**
DPC-4	**38.4**	**1123**	**65**	**0.06**	**0.0511**	**0.0010**	**0.2456**	**0.0052**	**0.0348**	**0.0005**	**247**	**25**	**223**	**4**	**221**	**3**
DPC-5	**61.6**	**1719**	**269**	**0.16**	**0.0530**	**0.0014**	**0.2546**	**0.0059**	**0.0349**	**0.0005**	**328**	**63**	**230**	**5**	**221**	**3**
DPC-6	**76.6**	**2200**	**306**	**0.14**	**0.0521**	**0.0009**	**0.2486**	**0.0046**	**0.0346**	**0.0005**	**288**	**20**	**225**	**4**	**219**	**3**
DPC-7	**48.9**	**1363**	**184**	**0.14**	**0.0536**	**0.0016**	**0.2518**	**0.0068**	**0.0341**	**0.0005**	**352**	**70**	**228**	**5**	**216**	**3**
DPC-8	**36.0**	**1006**	**157**	**0.16**	**0.0523**	**0.0012**	**0.2553**	**0.0061**	**0.0354**	**0.0005**	**298**	**29**	**231**	**5**	**224**	**3**
DPC-9	**34.5**	**949**	**247**	**0.26**	**0.0530**	**0.0018**	**0.2518**	**0.0075**	**0.0345**	**0.0005**	**329**	**77**	**228**	**6**	**218**	**3**
DPC-10	**23.0**	**603**	**295**	**0.49**	**0.0513**	**0.0013**	**0.2451**	**0.0065**	**0.0347**	**0.0005**	**252**	**35**	**223**	**5**	**220**	**3**
DPC-11	**65.0**	**1677**	**321**	**0.19**	**0.0542**	**0.0021**	**0.2508**	**0.0089**	**0.0336**	**0.0005**	**381**	**88**	**227**	**7**	**213**	**3**
DPC-12	**29.8**	**829**	**204**	**0.25**	**0.0537**	**0.0018**	**0.2533**	**0.0074**	**0.0342**	**0.0005**	**359**	**75**	**229**	**6**	**217**	**3**
DPC-13	**29.5**	**826**	**170**	**0.21**	**0.0537**	**0.0011**	**0.2565**	**0.0057**	**0.0346**	**0.0005**	**360**	**26**	**232**	**5**	**219**	**3**
DPC-14	**39.0**	**1074**	**244**	**0.23**	**0.0520**	**0.0018**	**0.2444**	**0.0075**	**0.0341**	**0.0005**	**283**	**79**	**222**	**6**	**216**	**3**
DPC-15	**76.4**	**1867**	**212**	**0.11**	**0.0526**	**0.0023**	**0.2505**	**0.0103**	**0.0346**	**0.0005**	**310**	**102**	**227**	**8**	**219**	**3**

(continued)

DPC-16	**51.8**	**1434**	**239**	**0.17**	**0.0530**	**0.0017**	**0.2532**	**0.0072**	**0.0346**	**0.0005**	**331**	**74**	**229**	**6**	**219**	**3**
DPC-17	**61.9**	**1732**	**210**	**0.12**	**0.0518**	**0.0016**	**0.2450**	**0.0065**	**0.0343**	**0.0005**	**277**	**70**	**222**	**5**	**217**	**3**
DPC-18	**50.0**	**1384**	**232**	**0.17**	**0.0529**	**0.0016**	**0.2518**	**0.0068**	**0.0345**	**0.0005**	**323**	**71**	**228**	**6**	**219**	**3**
DPC-19	**58.1**	**1684**	**176**	**0.10**	**0.0520**	**0.0009**	**0.2484**	**0.0048**	**0.0346**	**0.0005**	**287**	**21**	**225**	**4**	**219**	**3**
DPC-20	**24.9**	**714**	**78**	**0.11**	**0.0525**	**0.0017**	**0.2509**	**0.0070**	**0.0346**	**0.0005**	**309**	**74**	**227**	**6**	**220**	**3**

Table 2 Major (wt.%) and trace element concentrations (ppm) of the Luchuba and Wuchaba pluton.

	Luchuba pluton								Wuchaba pluton			
Sample	**SEB12-01**	**SEB12-02**	**BSB12-01**	**YDB12-03**	**YDB12-05**	**NSC12-01**	**TJZ12-01**	**LTB12-01**	**ZKL12-01**	**DBQ12-01**	**DBQ12-03**	**ZTC12-01**
Major elements (wt.%)												
SiO_2	**65.20**	**64.15**	**66.63**	**66.75**	**67.18**	**71.29**	**69.94**	**70.51**	**75.28**	**69.92**	**70.03**	**68.95**
TiO_2	**0.60**	**0.59**	**0.50**	**0.55**	**0.50**	**0.28**	**0.30**	**0.31**	**0.05**	**0.35**	**0.40**	**0.38**
Al_2O_3	**14.98**	**15.66**	**15.74**	**15.04**	**15.28**	**14.64**	**14.91**	**14.53**	**13.78**	**14.90**	**14.29**	**15.38**
TFe_2O_3	**4.41**	**4.12**	**3.40**	**3.92**	**3.44**	**1.81**	**1.93**	**2.28**	**0.85**	**2.54**	**2.97**	**2.76**
MnO	**0.07**	**0.06**	**0.06**	**0.07**	**0.06**	**0.04**	**0.04**	**0.04**	**0.02**	**0.05**	**0.06**	**0.06**
MgO	**2.64**	**2.77**	**1.66**	**2.58**	**1.70**	**0.77**	**0.88**	**0.99**	**0.27**	**0.82**	**0.92**	**0.86**
CaO	**3.86**	**3.85**	**2.96**	**3.58**	**3.03**	**1.89**	**2.07**	**2.27**	**0.39**	**2.04**	**2.20**	**1.99**
Na_2O	**3.32**	**3.44**	**3.56**	**3.19**	**3.35**	**3.62**	**3.59**	**3.44**	**3.72**	**3.15**	**3.04**	**3.26**
K_2O	**3.51**	**3.52**	**4.61**	**3.89**	**4.39**	**4.35**	**4.39**	**4.28**	**4.91**	**4.96**	**4.12**	**4.84**
P_2O_5	**0.17**	**0.16**	**0.18**	**0.14**	**0.22**	**0.08**	**0.14**	**0.10**	**0.11**	**0.12**	**0.18**	**0.14**
LOI	**0.66**	**1.34**	**0.43**	**0.87**	**0.74**	**0.87**	**0.74**	**0.44**	**0.56**	**0.38**	**0.85**	**0.73**
Na_2O+K_2O	**6.83**	**6.96**	**8.17**	**7.08**	**7.74**	**7.96**	**7.97**	**7.73**	**8.63**	**8.11**	**7.16**	**8.10**
K_2O/Na_2O	**1.06**	**1.02**	**1.29**	**1.22**	**1.31**	**1.20**	**1.22**	**1.24**	**1.32**	**1.58**	**1.36**	**1.48**
A/CNK	**0.97**	**1.01**	**0.97**	**0.98**	**0.98**	**1.01**	**1.01**	**1.00**	**1.03**	**1.00**	**1.04**	**1.04**
Total	**99.43**	**99.66**	**99.75**	**100.58**	**99.90**	**99.63**	**98.92**	**99.20**	**99.93**	**99.24**	**99.08**	**99.36**
Trace elements (ppm)												
Li	**68.8**	**18.7**	**87.1**	**80.4**	**78.0**	**104**	**121**	**110**	**22.9**	**83.9**	**90.5**	**80.4**
P	**657**	**590**	**736**	**699**	**713**	**302**	**430**	**443**	**255**	**571**	**588**	**562**
K	**36140**	**34200**	**41520**	**44800**	**42580**	**35760**	**40580**	**42140**	**49860**	**57740**	**42360**	**50540**
Sc	**10.4**	**10.1**	**7.03**	**10.2**	**8.08**	**3.54**	**5.26**	**4.93**	**2.96**	**5.33**	**6.17**	**5.74**
Ti	**4368**	**4080**	**3276**	**4448**	**3558**	**1742**	**2080**	**2108**	**316**	**2846**	**2916**	**2722**

(continued)

V	**85.0**	**76.4**	**54.2**	**80.8**	**62.3**	**25.1**	**66.0**	**31.5**	**3.65**	**32.9**	**33.9**	**31.5**
Cr	**109**	**115**	**46.2**	**103**	**49.8**	**18.0**	**22.1**	**22.3**	**2.89**	**11.1**	**11.5**	**11.4**
Mn	**588**	**441**	**476**	**574**	**503**	**289**	**356**	**336**	**119**	**491**	**532**	**499**
Co	**12.3**	**10.0**	**7.47**	**11.6**	**8.71**	**3.21**	**3.66**	**4.22**	**0.31**	**4.34**	**4.40**	**4.30**
Ni	**26.4**	**34.1**	**11.2**	**24.5**	**13.3**	**5.63**	**7.97**	**6.05**	**1.24**	**3.26**	**3.54**	**3.57**
Cu	**11.4**	**3.79**	**4.09**	**7.07**	**11.0**	**1.20**	**1.38**	**2.41**	**1.11**	**1.06**	**1.76**	**1.94**
Zn	**68.6**	**53.0**	**52.0**	**49.4**	**50.7**	**40.5**	**38.6**	**41.8**	**30.5**	**45.2**	**63.1**	**69.7**
Ga	**21.9**	**20.0**	**18.5**	**20.0**	**20.9**	**19.7**	**20.9**	**20.1**	**18.3**	**22.3**	**20.7**	**21.2**
Rb	**167**	**144**	**173**	**165**	**208**	**184**	**213**	**215**	**254**	**276**	**257**	**234**
Sr	**407**	**383**	**372**	**381**	**416**	**224**	**279**	**287**	**70.0**	**374**	**289**	**377**
Y	**17.3**	**17.7**	**14.9**	**15.7**	**17.1**	**10.9**	**13.5**	**12.8**	**17.0**	**20.1**	**20.8**	**16.1**
Zr	**198**	**190**	**121**	**173**	**196**	**121**	**140**	**122**	**45.9**	**214**	**194**	**173**
Nb	**16.5**	**15.1**	**14.0**	**14.1**	**15.7**	**14.5**	**16.0**	**14.4**	**11.1**	**20.1**	**22.0**	**17.9**
Cs	**12.8**	**8.92**	**9.58**	**12.6**	**13.5**	**15.9**	**18.5**	**15.9**	**20.0**	**15.7**	**21.7**	**14.8**
Ba	**874**	**879**	**815**	**834**	**875**	**458**	**559**	**697**	**270**	**1042**	**579**	**963**
La	**35.3**	**35.5**	**24.4**	**35.7**	**39.0**	**29.1**	**25.3**	**28.9**	**10.6**	**35.5**	**44.9**	**30.9**
Ce	**71.2**	**67.8**	**61.8**	**69.2**	**73.1**	**54.7**	**46.3**	**55.5**	**21.9**	**68.9**	**88.0**	**65.6**
Pr	**7.55**	**7.49**	**5.53**	**7.16**	**7.87**	**5.72**	**5.20**	**5.84**	**2.39**	**7.58**	**9.34**	**6.59**
Nd	**27.5**	**27.6**	**20.3**	**25.6**	**28.6**	**20.2**	**18.9**	**20.8**	**8.73**	**27.9**	**33.8**	**24.0**
Sm	**5.11**	**5.12**	**4.12**	**4.63**	**5.27**	**3.77**	**3.79**	**3.96**	**2.31**	**5.51**	**6.32**	**4.74**
Eu	**1.22**	**1.19**	**1.06**	**1.10**	**1.23**	**0.686**	**0.881**	**0.888**	**0.327**	**1.34**	**1.00**	**1.27**
Gd	**4.36**	**4.34**	**3.55**	**3.97**	**4.45**	**3.04**	**3.26**	**3.27**	**2.50**	**4.72**	**5.32**	**4.11**
Tb	**0.58**	**0.57**	**0.48**	**0.52**	**0.59**	**0.39**	**0.45**	**0.43**	**0.45**	**0.64**	**0.70**	**0.55**
Dy	**3.18**	**3.16**	**2.64**	**2.91**	**3.15**	**2.00**	**2.41**	**2.28**	**2.77**	**3.47**	**3.75**	**2.95**
Ho	**0.61**	**0.61**	**0.50**	**0.56**	**0.60**	**0.36**	**0.45**	**0.42**	**0.53**	**0.67**	**0.69**	**0.54**

(continued)

Er	**1.77**	**1.78**	**1.39**	**1.63**	**1.66**	**1.00**	**1.26**	**1.22**	**1.54**	**1.94**	**1.99**	**1.55**
Tm	**0.24**	**0.25**	**0.20**	**0.22**	**0.24**	**0.14**	**0.18**	**0.17**	**0.23**	**0.28**	**0.27**	**0.21**
Yb	**1.58**	**1.61**	**1.30**	**1.48**	**1.48**	**0.89**	**1.17**	**1.12**	**1.45**	**1.86**	**1.79**	**1.36**
Lu	**0.23**	**0.24**	**0.19**	**0.22**	**0.23**	**0.13**	**0.17**	**0.17**	**0.21**	**0.28**	**0.26**	**0.20**
Hf	**4.95**	**4.53**	**3.07**	**4.35**	**4.62**	**3.23**	**3.76**	**3.31**	**1.60**	**5.21**	**4.76**	**4.27**
Ta	**1.02**	**0.94**	**0.95**	**1.08**	**0.96**	**0.90**	**1.25**	**1.23**	**1.06**	**1.35**	**1.32**	**1.03**
Pb	**25.7**	**20.8**	**26.4**	**24.5**	**28.1**	**34.1**	**34.0**	**35.1**	**52.1**	**33.0**	**27.7**	**30.7**
Th	**15.9**	**14.5**	**15.8**	**14.7**	**16.5**	**17.3**	**16.4**	**15.7**	**7.3**	**17.4**	**21.3**	**17.3**
U	**4.20**	**3.68**	**3.33**	**2.30**	**5.79**	**7.74**	**3.70**	**4.13**	**3.84**	**12.0**	**10.3**	**4.31**
LREEs/HREEs	**4.96**	**4.78**	**4.67**	**5.26**	**5.26**	**6.05**	**4.40**	**5.29**	**1.74**	**4.33**	**5.15**	**4.83**
Eu/Eu*	**0.77**	**0.75**	**0.83**	**0.77**	**0.76**	**0.60**	**0.75**	**0.73**	**0.41**	**0.78**	**0.51**	**0.86**
$(La/Yb)_N$	**16.07**	**15.85**	**13.46**	**17.27**	**18.84**	**23.55**	**15.57**	**18.47**	**5.281**	**13.72**	**17.98**	**16.25**
Sr/Y	**23.58**	**21.61**	**25.06**	**24.23**	**24.39**	**20.55**	**20.70**	**22.42**	**4.12**	**18.66**	**13.88**	**23.48**
Nb/Ta	**16.17**	**16.12**	**14.64**	**13.04**	**16.43**	**16.08**	**12.80**	**11.76**	**10.46**	**14.88**	**16.67**	**17.31**
						Wuchaba pluton						
Sample	**XJB12-01**	**MDG12-01**	**MXB12-02**	**MXB12-03**	**DPC12-01**	**DBL12-01**	**MZG12-02**	**CJM12-01 (host)**	**CJM12-01 (MME)**	**CJM12-03**	**MK12-02**	**MK12-04**
Major elements (wt.%)												
SiO_2	**72.25**	**71.28**	**71.74**	**73.61**	**70.64**	**70.56**	**64.61**	**72.08**	**53.31**	**73.91**	**68.35**	**53.92**
TiO_2	**0.31**	**0.36**	**0.29**	**0.18**	**0.29**	**0.39**	**0.51**	**0.38**	**1.06**	**0.05**	**0.46**	**1.02**
Al_2O_3	**14.40**	**14.31**	**14.65**	**14.38**	**15.24**	**14.67**	**16.79**	**13.77**	**16.70**	**13.86**	**14.88**	**16.28**
TFe_2O_3	**2.09**	**2.30**	**1.75**	**1.52**	**2.11**	**2.60**	**3.51**	**2.54**	**9.52**	**0.48**	**3.39**	**7.89**
MnO	**0.06**	**0.06**	**0.03**	**0.02**	**0.04**	**0.05**	**0.08**	**0.06**	**0.28**	**0.03**	**0.07**	**0.17**
MgO	**0.60**	**0.73**	**0.48**	**0.31**	**0.54**	**0.87**	**1.05**	**0.83**	**3.48**	**0.12**	**1.08**	**3.73**
CaO	**1.55**	**1.84**	**0.97**	**0.96**	**1.34**	**1.85**	**1.67**	**3.07**	**4.69**	**0.90**	**2.62**	**4.81**

(continued)

Na_2O	**3.52**	**3.42**	**3.47**	**3.48**	**3.69**	**3.46**	**3.19**	**3.98**	**3.43**	**4.00**	**3.43**	**3.17**
K_2O	**4.55**	**4.18**	**4.92**	**4.50**	**4.43**	**3.84**	**7.27**	**1.88**	**5.82**	**4.97**	**3.99**	**6.09**
P_2O_5	**0.12**	**0.15**	**0.12**	**0.13**	**0.11**	**0.16**	**0.20**	**0.18**	**0.39**	**0.04**	**0.13**	**0.56**
LOI	**0.45**	**0.74**	**0.81**	**1.42**	**0.66**	**0.73**	**0.78**	**0.42**	**0.51**	**0.72**	**0.76**	**0.76**
Na_2O+K_2O	**8.07**	**7.59**	**8.39**	**7.99**	**8.12**	**7.30**	**10.47**	**5.86**	**9.25**	**8.97**	**7.43**	**9.26**
K_2O/Na_2O	**1.29**	**1.22**	**1.42**	**1.29**	**1.20**	**1.11**	**2.28**	**0.47**	**1.70**	**1.24**	**1.16**	**1.92**
A/CNK	**1.02**	**1.03**	**1.06**	**1.09**	**1.09**	**1.10**	**0.93**	**1.09**	**0.82**	**0.95**	**1.02**	**0.97**
Total	**99.91**	**99.37**	**99.24**	**100.52**	**99.10**	**99.17**	**99.68**	**99.18**	**99.18**	**99.07**	**99.16**	**98.39**
Trace elements (ppm)												
Li	**123**	**117**	**140**	**62.9**	**131**	**77.5**	**106**	**47.1**	**134**	**46.4**	**120**	**168**
P	**444**	**467**	**464**	**288**	**492**	**544**	**752**	**523**	**1753**	**100**	**687**	**2381**
K	**40940**	**45080**	**47500**	**46920**	**44060**	**37700**	**68560**	**16512**	**65860**	**46060**	**41440**	**57344**
Sc	**4.55**	**4.97**	**2.91**	**2.42**	**3.66**	**4.59**	**6.67**	**6.88**	**23.3**	**2.25**	**6.62**	**17.1**
Ti	**2126**	**2584**	**1909**	**1229**	**2006**	**2662**	**3608**	**2428**	**7912**	**325.2**	**3338**	**6897**
V	**21.5**	**27.1**	**15.9**	**9.25**	**16.1**	**29.6**	**42.3**	**30.3**	**154**	**1.91**	**40.9**	**161**
Cr	**9.88**	**11.5**	**4.86**	**4.60**	**21.3**	**13.7**	**14.8**	**11.9**	**77.1**	**2.58**	**14.8**	**17.5**
Mn	**455**	**484**	**243**	**178**	**337**	**396**	**638**	**439**	**2422**	**202**	**583**	**1377**
Co	**3.10**	**3.86**	**2.13**	**1.33**	**2.70**	**4.35**	**5.59**	**3.75**	**17.1**	**0.08**	**5.21**	**18.4**
Ni	**3.56**	**4.73**	**3.55**	**2.13**	**13.1**	**6.46**	**5.96**	**3.56**	**16.0**	**1.29**	**5.33**	**8.40**
Cu	**1.47**	**2.62**	**1.63**	**1.76**	**2.86**	**4.08**	**2.22**	**2.94**	**66.1**	**0.585**	**3.29**	**3.56**
Zn	**61.5**	**54.8**	**78.7**	**106**	**58.0**	**63.0**	**98.5**	**58.0**	**160**	**22.9**	**76.1**	**101**
Ga	**21.4**	**23.1**	**25.4**	**25.6**	**25.9**	**21.9**	**23.6**	**19.9**	**25.5**	**19.6**	**23.3**	**18.8**
Rb	**271**	**257**	**310**	**295**	**283**	**215**	**341**	**113**	**368**	**339**	**261**	**328**
Sr	**234**	**313**	**184**	**146**	**215**	**303**	**364**	**315**	**226**	**32.6**	**329**	**428**
Y	**22.3**	**16.9**	**9.48**	**9.46**	**15.0**	**16.1**	**22.4**	**19.6**	**50.0**	**17.9**	**26.8**	**27.7**

(continued)

Zr	**144**	**155**	**166**	**121**	**160**	**195**	**256**	**197**	**220**	**43.6**	**227**	**216**
Nb	**21.5**	**21.0**	**20.3**	**21.8**	**23.0**	**19.9**	**25.9**	**17.4**	**31.6**	**17.6**	**26.2**	**15.3**
Cs	**21.9**	**23.6**	**26.5**	**13.5**	**20.8**	**13.0**	**13.9**	**9.55**	**24.9**	**44.3**	**22.8**	**13.3**
Ba	**534**	**782**	**628**	**491**	**620**	**729**	**1222**	**245**	**541**	**38.3**	**661**	**846**
La	**30.6**	**31.8**	**34.6**	**28.6**	**35.6**	**26.2**	**63.8**	**38.1**	**34.8**	**8.96**	**36.9**	**36.3**
Ce	**59.2**	**59.4**	**70.0**	**55.9**	**68.6**	**59.4**	**119**	**73.1**	**69.6**	**19.1**	**71.1**	**75.6**
Pr	**6.51**	**6.38**	**7.20**	**5.95**	**7.29**	**5.50**	**12.89**	**7.88**	**8.61**	**2.13**	**7.93**	**9.18**
Nd	**23.8**	**22.6**	**25.3**	**20.8**	**25.9**	**19.9**	**45.5**	**28.9**	**36.6**	**7.74**	**29.5**	**36.4**
Sm	**4.95**	**4.47**	**4.68**	**3.98**	**4.90**	**4.15**	**7.87**	**5.70**	**10.47**	**2.38**	**6.25**	**7.69**
Eu	**0.82**	**0.93**	**0.79**	**0.65**	**0.83**	**0.83**	**1.34**	**0.95**	**0.93**	**0.14**	**1.08**	**1.60**
Gd	**4.40**	**3.94**	**3.45**	**3.04**	**3.96**	**3.66**	**6.14**	**4.99**	**10.9**	**2.69**	**5.65**	**7.14**
Tb	**0.64**	**0.56**	**0.40**	**0.37**	**0.53**	**0.51**	**0.76**	**0.67**	**1.65**	**0.49**	**0.80**	**0.96**
Dy	**3.67**	**3.09**	**1.91**	**1.83**	**2.71**	**2.86**	**3.94**	**3.58**	**9.53**	**2.95**	**4.52**	**5.06**
Ho	**0.70**	**0.57**	**0.32**	**0.31**	**0.49**	**0.53**	**0.73**	**0.66**	**1.78**	**0.56**	**0.87**	**0.93**
Er	**2.12**	**1.60**	**0.85**	**0.84**	**1.37**	**1.51**	**2.11**	**1.87**	**5.01**	**1.62**	**2.55**	**2.48**
Tm	**0.32**	**0.22**	**0.11**	**0.11**	**0.20**	**0.21**	**0.29**	**0.25**	**0.67**	**0.24**	**0.37**	**0.33**
Yb	**2.18**	**1.43**	**0.72**	**0.72**	**1.25**	**1.37**	**1.87**	**1.61**	**4.30**	**1.56**	**2.45**	**2.16**
Lu	**0.32**	**0.21**	**0.10**	**0.10**	**0.19**	**0.20**	**0.28**	**0.24**	**0.62**	**0.22**	**0.36**	**0.32**
Hf	**3.95**	**3.94**	**4.18**	**3.28**	**4.11**	**4.58**	**6.11**	**4.74**	**5.17**	**1.63**	**5.56**	**4.84**
Ta	**2.04**	**1.55**	**1.30**	**1.65**	**1.78**	**1.34**	**1.61**	**1.04**	**1.80**	**1.70**	**1.85**	**0.88**
Pb	**34.8**	**34.6**	**31.2**	**39.3**	**35.0**	**29.5**	**40.7**	**18.9**	**41.5**	**59.2**	**32.5**	**29.5**
Th	**18.4**	**14.7**	**18.7**	**15.6**	**19.8**	**14.9**	**29.8**	**17.1**	**9.2**	**6.5**	**18.5**	**8.88**
U	**3.76**	**4.23**	**4.14**	**4.86**	**2.93**	**3.75**	**5.48**	**6.43**	**6.50**	**4.58**	**6.50**	**2.45**
LREEs/HREEs	**3.43**	**4.40**	**8.22**	**6.91**	**5.57**	**4.30**	**6.49**	**4.63**	**1.90**	**1.44**	**3.45**	**3.55**

(continued)

Eu/Eu*	**0.52**	**0.66**	**0.58**	**0.55**	**0.56**	**0.63**	**0.57**	**0.53**	**0.26**	**0.16**	**0.54**	**0.65**
$(La/Yb)_N$	**10.07**	**15.97**	**34.61**	**28.64**	**20.48**	**13.73**	**24.48**	**16.96**	**5.80**	**4.13**	**10.80**	**12.03**
Sr/Y	**10.47**	**18.52**	**19.41**	**15.41**	**14.34**	**18.80**	**16.21**	**16.13**	**4.52**	**1.82**	**12.29**	**15.47**
Nb/Ta	**10.56**	**13.59**	**15.66**	**13.22**	**12.92**	**14.87**	**16.06**	**16.70**	**17.52**	**10.34**	**14.18**	**17.38**

A/CNK = molar $Al_2O_3/(CaO + Na_2O+K_2O)$; A/NK = molar $Al_2O_3/(Na_2O+K_2O)$; Eu/Eu* =$W(Eu)_N/[(1/2)(W(Sm)_N +W(Gd)_N)]$; $(La/Yb)_N$ is normalized by Chondrite, Chondrite values are from Sun and McDonough (1989).

Table 3 Sr, Nd, Hf isotopes of the Luchuba and Wuchaba pluton.

Sample	$^{87}Rb/^{86}Sr$	$^{87}Sr/^{86}Sr$	2σSE	$I_{Sr}(t)$	$^{147}Sm/^{144}Nd$	$^{143}Nd/^{144}Nd$	2σSE	$\varepsilon_{Nd}(t)$	$^{176}Lu/^{177}Hf$	$^{176}Hf/^{177}Hf$	2σSE	$\varepsilon_{Hf}(t)$
SEB12-01	1.18	0.711734	0.000006	0.7080	0.113	0.512173	0.000003	-6.72	0.006652	0.282595	0.000005	-2.40
BSB12-01	1.33	0.712454	0.000005	0.7083	0.124	0.512228	0.000004	-5.95	0.008734	0.282623	0.000006	-1.71
YDB12-03	1.24	0.712255	0.000005	0.7084	0.110	0.512170	0.000004	-6.69	0.007063	0.282587	0.000005	-2.74
YDB12-05	1.44	0.712253	0.000006	0.7077	0.112	0.512223	0.000003	-5.73	0.007126	0.282618	0.000003	-1.65
LTB12-01	2.16	0.717152	0.000006	0.7104	0.116	0.512150	0.000004	-7.25	0.007290	0.282567	0.000006	-3.48
ZKL12-01	10.50	0.737981	0.000016	0.7051	0.161	0.512171	0.000003	-8.11	0.018453	0.282522	0.000005	-6.70
DBQ12-01	2.14	0.713920	0.000006	0.7072	0.120	0.512218	0.000009	-6.05	0.007603	0.282613	0.000007	-1.90
MXB12-02	4.85	0.723182	0.000006	0.7080	0.112	0.512171	0.000009	-6.74	0.003485	0.282592	0.000005	-2.04
DPC12-01	3.81	0.719421	0.000006	0.7075	0.115	0.512163	0.000009	-6.98	0.006547	0.282606	0.000003	-1.99
MZG12-02	2.71	0.715710	0.000017	0.7072	0.105	0.512220	0.000011	-5.59	0.006554	0.282602	0.000005	-2.13
CJM12-01(host)	1.04	0.711114	0.000008	0.7079	0.120	0.512245	0.000010	-5.52	0.007084	0.282614	0.000006	-1.79
CJM12-01(MME)	4.70	0.721585	0.000005	0.7069	0.174	0.512363	0.000008	-4.74	0.016965	0.282683	0.000006	-0.78
CJM12-03	30.07	0.785554	—	—	0.187	0.512119	0.000012	-9.86	0.019316	0.282554	0.000006	-5.69
MK12-02	2.28	0.714738	0.000005	0.7076	0.129	0.512285	0.000008	-4.98	0.009231	0.282625	0.000005	-1.71
MK12-04	2.22	0.714264	0.000006	0.7073	0.129	0.512369	0.000007	-3.34	0.009248	0.282718	0.000006	1.58

Where, t=crystallization time of zircon (~220 Ma).$^{87}Rb/^{86}Sr$,$^{147}Sm/^{144}Nd$,$^{176}Lu/^{177}Hf$ ratios calculated using Rb, Sr, Sm and Nd contents, measured by ICP-MS.

$(^{147}Sm/^{144}Nd)_{CHUR}$=0.1967, $(^{143}Nd/^{144}Nd)_{CHUR}$=0.512638;$(^{176}Lu/^{177}Hf)_{CHUR}$=0.0332, $(^{176}Hf/^{177}Hf)_{CHUR}$=0.282772 (Blichert-Toft and Albarède, 1997).